In this chapter we must come to grips with how tectonics works. We must get specific about what a plate is, and why it moves at rates of the order of centimeters per year. This in turn will serve to introduce the two major means by which heat moves about within the Earth – conduction (to create the lithosphere) and convection (to move the lithospheric plates about). We will also address the mechanisms by which large-scale topographic loads (continents, ice sheets, large lakes) are supported – by buoyancy. Indeed, while the support of such large static loads is associated with the density contrast of the materials involved, changes in loads such as ice sheets and lakes can incite a mantle response that determines the timescale for the response of the Earth. It is in this way that the study of geomorphology, and in particular documentation of the deformation rates one can deduce from deformed geomorphic markers such as shorelines, can provide some of the strongest constraints on mantle rheology.

We cannot begin to discuss the topography of the Earth and the processes responsible for modifying it before outlining first how plate tectonics works. The broadest outlines of the Earth's topography are all connected to plate tectonics: the mountain chains that reflect both the spreading centers and the subduction zones, the organized bathymetry of the ocean basins separating the ridges from the subduction zones, the highest topography associated with continent–continent collisions, and even the volcanic hot spot tracks all owe their patterns to the motions of lithospheric plates that comprise the exterior carapace of the Earth. We first discuss what the plates are: the lithosphere is simply the conductively cooled thermal boundary layer at the top of the mantle. This fact has tremendous leverage in allowing us to understand the bathymetry of ocean basins. We then describe briefly the process by which plates move, with the target of understanding quantitatively the plate speeds of roughly 10 cm/yr.

Ocean basins: the marriage of conduction and isostasy

Beyond the basic oblate spheroidal shape of the Earth discussed in Chapter 2, the second largest topographic features on Earth are its ocean basins. Since beginning to collect very detailed bathymetric information in the 1930s, we have learned that the ocean basins are remarkably well organized. In particular, each major basin has a topographic high, away from which the elevations of the sea floor fall off with considerable regularity. The pattern is quite visible in Figure 3.1. This gross structure of the ocean floor has since been explained by recognition of these topographic highs, or mid-ocean ridges, as spreading centers, where mantle is welling up, partially melted by pressure-release to produce oceanic crust consisting largely of basalts. This thin (roughly 5 km thick) scum of crust is wafted away from the spreading center at a rate of a few centimeters per year. On closer inspection, the decay from the heights of the mid-ocean ridges to the depths of the abyssal plains is remarkably similar from place to place. Why does the bathymetry display this regular pattern? First, what do the data say?

As shown in Figure 3.2, the bathymetry looks similar from basin to basin when plotted not against distance from the ridge, but as elevation vs. *age* of crust. It falls off first rapidly, then more and more slowly with age. We can investigate what sorts of mathematical functions best fit this pattern. If we expect that this pattern is a power law, we might plot the elevation vs. distance on log–log paper, while if we expect that it is exponential, we would choose semi-log paper (see Math appendix). When this is done, it appears that the pattern is well fit with a power of about 1/2. The formula for the bathymetry shown in either of these two basins is therefore

$$D = D_0 + a\sqrt{t} \tag{3.1}$$

where D is ocean depth, D_0 is the depth at the spreading center, t is the age of the plate at some distance x, and a is a constant. Clearly, we can substitute $x/(u/2)$ for the age as long as we know the half-spreading rate, $u/2$. Why should ocean depth increase as the square root of the age of the lithosphere? That this phenomenon so clearly displays a square root of time dependence cries out for a physical explanation. The answer lies in the thermal evolution of the oceanic lithosphere.

As the plate moves away from the spreading center, it thickens. But what defines the "plate" and why does it thicken? There are several ways to think about it: (1) it is all that material at depth that moves with the surface, (2) it is all that material that behaves as a solid on geological timescales (millions of years). In either instance, note that the definition is one based not on compositional differences (as for instance the Moho at the base of the oceanic crust is defined).

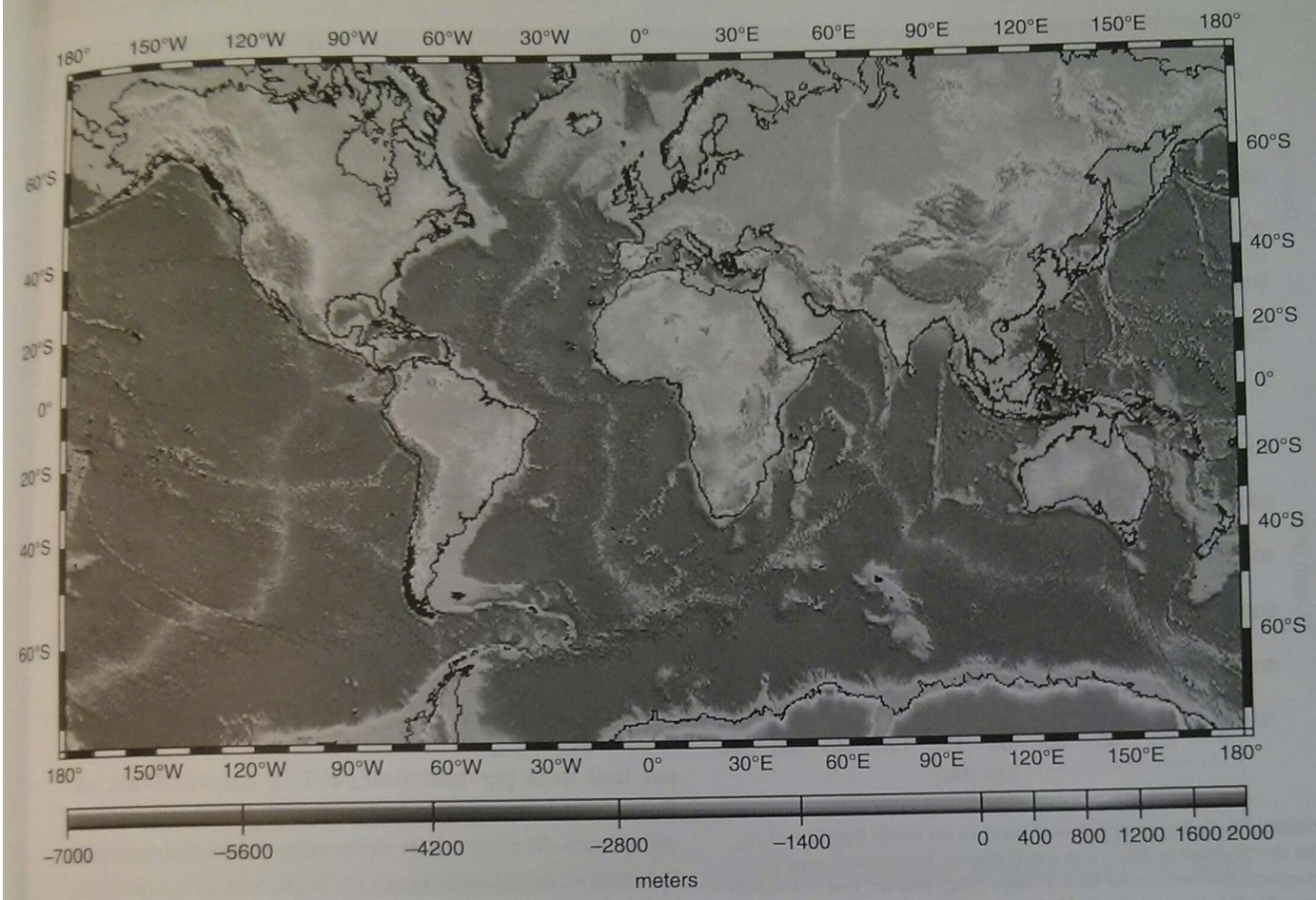

Figure 3.1 Global topography showing both ocean bathymetry and land elevations. Ocean bathymetry reveals orderly increase in depth away from major spreading centers, e.g., the mid-Atlantic Ridge. Note also the continental shelves. (source: http://www.ldeo.columbia.edu/~small/GDEM.html, 2′ Digital Elevation Model generated by D. T. Sandwell, W. H. F. Smith, and C. Small. Continental elevations derived from EROS GTOPO30 DEM. Submarine elevations based on Scripps/NOAA predicted bathymetry derived from Geosat, ERS-1, and Topex/Poseidon Satellite altimetry).

but on material behavior differences. *The lithosphere is a rheological boundary layer*. The rheology of a material, derived from the Greek rhein for "to flow," describes the rate and style of deformation of that material under stress. The main determinant of the rheology of the mantle is its temperature. This means that we can think of the lithosphere as a thermal boundary layer as well as a rheological one. But what is meant by this fancy phrase "boundary layer"? We will see it several times in geomorphology. Most generally, it is a region close to the surface of some object in which some property changes dramatically. Here the surface is the bottom of the ocean, the object is the Earth, and the property undergoing rapid or large-scale change is the temperature. As another example, we also live in the atmospheric boundary layer, the base of the atmosphere where one of several properties changing rapidly is the wind velocity. It is zero at the ground surface and changes rapidly within the bottom kilometer, even in the bottom few meters. The other edge of a boundary layer is often arbitrary. In the case of the lithosphere, we chose to take the bottom boundary of the lithosphere to be where the mantle has reached a temperature of about 1200 °C. This choice is based upon laboratory experiments that show that mantle materials above this temperature deform sufficiently rapidly to behave as fluids on geological timescales. So the base of the lithosphere is defined by an isotherm. We reiterate that the lithosphere, unlike the crust, is a layer defined by rheology, and not by composition.

Given the above discussion of the lithosphere, we see that the problem of the gross pattern of topography on the ocean floor is therefore transformed into a problem in heat flow. Here we introduce the

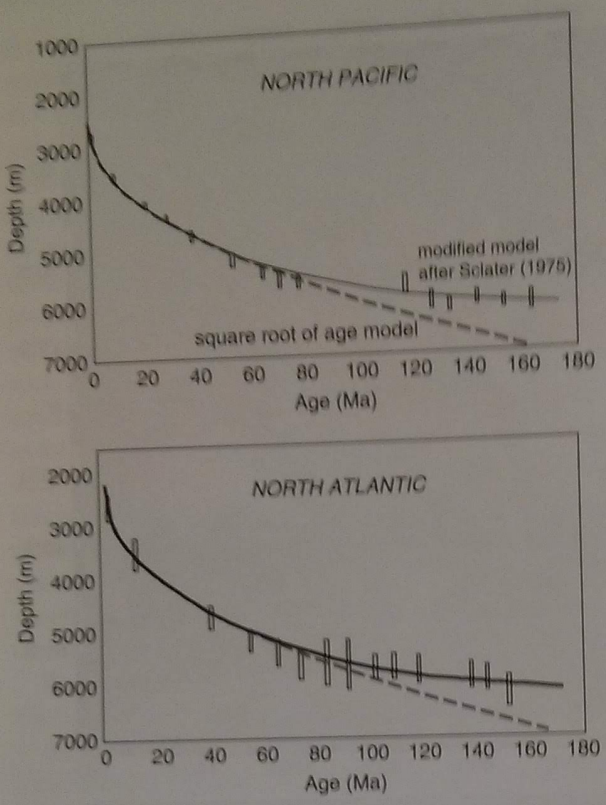

Figure 3.2 Bathymetry (vertical bars) of (a) North Pacific and (b) North Atlantic oceans as a function of lithospheric age, in transects perpendicular to the ridge crest. Dashed line is a model based upon the square root of lithospheric age, solid line is a modification of this from Sclater *et al.* (1975). Square root of age model works well out to roughly 80 Ma (redrawn from Parsons and Sclater, 1977, with permission from American Geophysical Union).

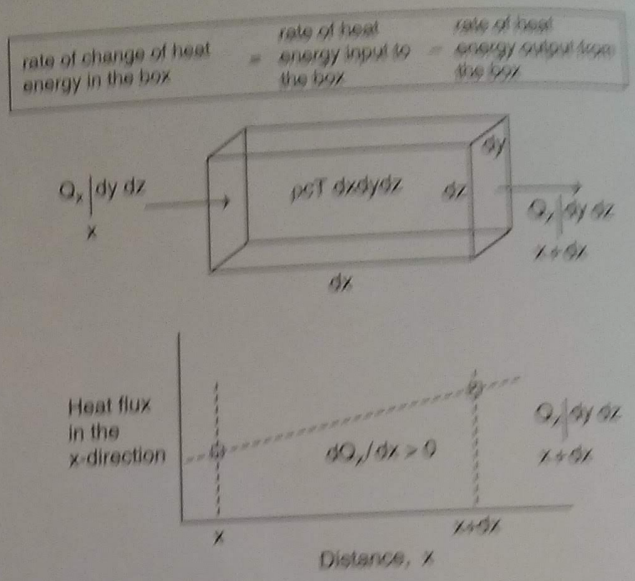

Figure 3.3 Word picture and box diagram required for derivation of heat flow equation.

concepts of heat conservation and conduction to treat this problem formally. The upwelling hot mantle material is roughly 1600 °C, while the ocean floor is very close to 0 °C. Ignoring for the moment the region very close to the spreading center, the principal means by which the near-surface rock is cooled is by conduction. Vibrational energy is traded off between adjacent atoms in such a way as to even out the energy, meaning that it flows from regions of high energy (temperature) to regions of low temperature. The result is a relationship that has become known as Fourier's law, where the flux of heat in a particular direction, say along the x-axis, is proportional to the local gradient of temperature in that direction, through a constant called the thermal conductivity, k:

$$Q_x = -k_x \frac{\partial T}{\partial x} \qquad (3.2)$$

This heat flux, Q, is defined as having units of energy per unit area per unit time, E/L^2T (in this book all fluxes will have units of something per unit area per unit time). We can then determine what the units of thermal conductivity must be to render the equation dimensionally correct. As the temperature gradient has units of degrees per unit distance (°T/L), k must have units of $(E/L^2T)/(°T/L) = E/°TLT$ or $(E/T)/°TL$. In SI units, in which lengths are in meters, masses in kilograms, and times in seconds (hence the old MKS system), this is W/m °C. The minus sign in Equation 3.2 assures that the heat travels *down* thermal gradients. We need to formalize one more concept, the conservation of energy. Consider a box of material depicted in Figure 3.3, and think about the quantity of thermal energy (heat) in the box. The conservation of heat can be written, in words:

> the rate of change of heat in the box = rate of input of heat into the box minus the rate of heat output from the box

To turn this word picture into a mathematical statement, we need expressions for each of the terms. The heat in the box is simply the temperature of the box (which we can think of as the concentration of heat per unit mass), times the mass per unit volume (the density) times the thermal heat capacity (energy per unit mass per degree of temperature): $H = \rho cT\,dx\,dy\,dz$.

Box 3.1 Using the Taylor series

We could arrive at the same differential equation using a different method. Consider again the fluxes of heat through the edges of the box. While we can assert the flux of heat at a position x, $Q(x)$, we required an expression for the flux of heat at the other side of the box, $Q(x + \mathrm{d}x)$. Recall from Appendix B the Taylor series representation for the value of a function at a new position given its value and its derivatives at a known position. Applying this to our situation, we have

$$Q(x+\mathrm{d}x) = Q(x) + \frac{1}{1!}\frac{\mathrm{d}Q}{\mathrm{d}x}\mathrm{d}x + \frac{1}{2!}\frac{\mathrm{d}^2Q}{\mathrm{d}x^2}\mathrm{d}x^2 + \cdots$$

In the one-dimensional heat balance, and ignoring sources and sinks of heat, we now have

$$\frac{\partial(\rho cT\mathrm{d}x\mathrm{d}y\mathrm{d}z)}{\partial t} = Q(x)\mathrm{d}y\mathrm{d}z - Q(x+\mathrm{d}x)\mathrm{d}y\mathrm{d}z$$

Representing $Q(x + \mathrm{d}x)$ with the Taylor series, and ignoring higher order terms, those with derivatives of second and higher order, which are multiplied by higher and higher powers of the small increment $\mathrm{d}x$, this becomes

$$\frac{\partial(\rho cT\mathrm{d}x\mathrm{d}y\mathrm{d}z)}{\partial t} = Q(x)\mathrm{d}y\mathrm{d}z - \left[Q(x) + \frac{\mathrm{d}Q}{\mathrm{d}x}\mathrm{d}x\right]\mathrm{d}y\mathrm{d}z = -\frac{\partial Q}{\partial x}\mathrm{d}x\mathrm{d}y\mathrm{d}z$$

Finally, dividing by $\rho c\mathrm{d}x\mathrm{d}y\mathrm{d}z$, we arrive at an equation for the evolution of temperature:

$$\frac{\partial T}{\partial t} = -\frac{1}{\rho c}\frac{\partial Q}{\partial x}$$

This is identical to Equation 3.5.

The rate of change of this quantity with time is therefore the left-hand side of the equation: $\frac{\partial(\rho cT\mathrm{d}x\mathrm{d}y\mathrm{d}z)}{\partial t}$. The rate at which heat is coming across the left-hand side of the box we denote $Q_x(x)\mathrm{d}y\mathrm{d}z$ (which reads "heat flux in the x-direction, evaluated at the location x") and that going out the right-hand side of the box is similarly $Q_x(x+\mathrm{d}x)\mathrm{d}y\mathrm{d}z$, or the heat flux evaluated at $x + \mathrm{d}x$. Our equation then becomes

$$\frac{\partial(\rho cT\mathrm{d}x\mathrm{d}y\mathrm{d}z)}{\partial t} = Q_x(x)\mathrm{d}y\mathrm{d}z - Q_x(x+\mathrm{d}x)\mathrm{d}y\mathrm{d}z \qquad (3.3)$$

Up to this point we have made very few assumptions. The only thing missing is any heat that is either produced or consumed within the box, which could happen by radioactive decay of elements, or strain heating of a fluid, or the change of phase of the material. We will ignore all of these for the present. The oceanic lithosphere is relatively poor in radioactive elements, meaning that we can safely ignore a radioactive heat source. For now we will also ignore the other potential heat sources. Now let's simplify this a little. We can hold the volume of material in this solid constant through time, allowing us to pull the $\mathrm{d}x$, $\mathrm{d}y$, and $\mathrm{d}z$ out of the partial derivative with respect to time. Let's also assume that the density and the heat capacity of the material don't change over the temperature range we are concerned with. When we divide both sides by $\rho c\mathrm{d}x\mathrm{d}y\mathrm{d}z$, the equation simplifies to

$$\frac{\partial T}{\partial t} = -\left(\frac{1}{\rho c}\right)\frac{[Q_x(x+\mathrm{d}x) - Q_x(x)]}{\mathrm{d}x} \qquad (3.4)$$

The last step involves the simple recognition that if we were to shrink the size of our box so that $\mathrm{d}x$ tends toward zero, the term in brackets on the right-hand side is the spatial derivative of the heat flux, $\partial Q_x/\partial x$ and the final equation for the conservation of heat becomes

$$\frac{\partial T}{\partial t} = -\left(\frac{1}{\rho c}\right)\frac{\partial Q_x}{\partial x} \qquad (3.5)$$

This equation says that the temperature in a region will rise if there is a negative gradient in the flux of heat across it, and vice versa. We have shown this in Figure 3.3. If there is a positive gradient in the x-direction, then more heat is leaving out the right-hand side of the box than is arriving through the left-hand side of the box, and the temperature in the box ought to decline.

Note that we have not yet specified the mechanism by which heat is transported across the edges of the box. In the case at hand, the cooling of the oceanic lithosphere, in which conduction is the primary mechanism of heat flow, we turn to the physics of conduction, and apply Equation 3.2, Fourier's law for conduction of heat, for the heat flux, Q_x. This results in

$$\frac{\partial T}{\partial t} = -\left(\frac{1}{\rho c}\right)\frac{\partial\left(-k\dfrac{\partial T}{\partial x}\right)}{\partial x} \tag{3.6}$$

Making the final assumption that the conductivity is uniform within the material and thus does not depend upon x, the conductivity can be removed from the x-derivative and the heat equation becomes

$$\frac{\partial T}{\partial t} = \kappa\frac{\partial^2 T}{\partial x^2} \tag{3.7}$$

where $\kappa = k/c\rho$ and is called the thermal diffusivity and has the simple units of length^2/time. Equation 3.7 is called the diffusion equation. We will see the diffusion equation in several contexts within this book. You have heard the adage that nature abhors vacuums. It also hates sharp corners in things. Diffusive processes destroy sharp corners by removing sharp peaks and filling in valleys. Equation 3.7 describes how diffusion smoothes the sharp step in the temperature profile of the oceanic lithosphere imposed by placing hot new material against cold seawater. We will also encounter the diffusion equation when we talk about the decay of sharp topography through time. Diffusion also describes the gradual decay of spikes in concentration of a chemical in a fluid, such as ink in water. In each of these examples, the transport of heat or soil or a chemical is driven by a conduction-like process, one in which flux of something is proportional to the gradient in that quantity. Peaks and valleys in concentration (of mass, heat, topography, ink ...) can be recognized by their curvature, or second derivative, peaks being high negative curvature, valleys positive. The rate of change of the temperature is dictated by the local curvature of the temperature profile, and by the thermal diffusivity.

Now let's return to the cooling of the oceanic lithosphere. Armed with this mathematical description of how conduction works, and mathematical statements that capture this physics, consider now the problem of how the oceanic lithosphere thickens with time. We simplify the problem to one in which a column of new crustal material of roughly uniform temperature is brought suddenly into contact along its top surface with the cold base of the ocean. The starting profile is uniform except at its very top surface. The ocean acts as a "boundary condition" in the problem. We also assume that the ocean so efficiently mixes that it does not warm up in the process (as might rock at the edge of a magma chamber, say). So, to a good approximation, the top boundary condition is held at a constant temperature, of say 4 °C. Given the word picture of how conduction works, think about what will happen to the temperatures in the column of rock. Consider a single parcel of rock just below the surface or box, and think about the fluxes of heat into and out of it. No heat flows into the base of it, as there is no thermal gradient driving the flux. This is definitely not the case at the top, where the top feels a huge thermal gradient, a very large temperature difference across a short distance. Heat therefore flows rapidly out the top of the box, and none flows in the base. By conservation of heat, the heat content of the box, and therefore the temperature of the box, declines. Now take a later snapshot of the thermal drama. The temperature of the box is now distinctly below its original temperature. There is therefore a thermal gradient driving flow toward it from the bottom. As well, there continues to be a large gradient driving flow out the top, although note that this gradient has now declined because the temperature of the box is now lower, and therefore closer to that of the top boundary, the ocean floor. So it ought to continue to cool, but at a lower rate. The temperature profiles through time will therefore evolve in the way we have depicted them in Figure 3.4. The depth to a particular isotherm increases rapidly at first, and more slowly thereafter. The formal solution for the depth, L, to a chosen temperature with time is

$$L = \eta\sqrt{\kappa t} \tag{3.8}$$

where the dimensionless factor η is of order unity (close to 1), and t is the time since the temperature at the surface was lowered. The depth in fact varies as *the square root of time*! This is a principal and very

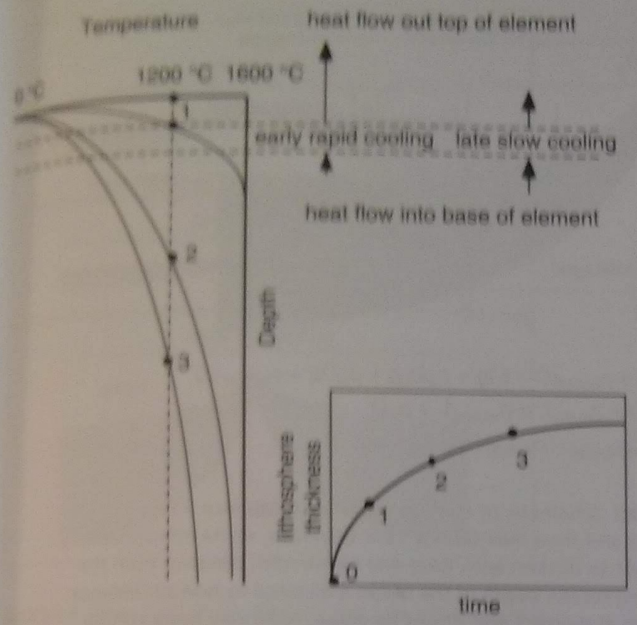

Figure 3.4 Evolution of thermal structure in a cooling column of rock. Initial temperature profile (bold line) of column at uniform temperature of 1600 °C. Subsequent to exposure at spreading ridge, top surface is held at 0 °C ocean bottom temperature. Temperature cools at all depths from time 1 through time 3. The 1200 °C isotherm, reflecting the rheological definition of the base of the lithosphere, deepens through time, from time 0 through time 3, as shown by dots at intersection with the temperature profile, and in lower right box. Heat flux into an element delineated by dashed lines shows large mismatch between heat flowing out top and into base at early times, changing to much lower mismatch at later times. The large mismatch in temperature causes rapid cooling in early times, decaying to slower cooling rates at later times.

useful result of diffusion problems: length scales and timescales are related through the simple formula $\delta \sim \sqrt{\kappa t}$ or $t \sim \delta^2/\kappa$, where δ is a length scale (say the distance from a boundary to a particular isotherm) and t is a timescale. The exact values depend upon the particular isotherm chosen, and the particular temperatures of the boundaries.

The bottom line, then, is that the physics of conductive cooling of a column of material subjected to a new and constant top temperature dictates that the oceanic lithosphere (remember, defined by an isotherm) thickens at a rate proportional to the square root of time. But why does the lithosphere droop into the underlying cooler mantle as it moves away from the spreading ridge? The reason is that it is denser than the underlying mantle because its mean temperature is lower than that of the underlying mantle. It wants to sink into the mantle, and the thicker it is the lower it sinks. Note that the lithosphere ultimately does founder entirely, at subduction zones. If we know what the mean density of the lithosphere is, then we can do another isostatic column balance to determine how low lithosphere of a given thickness ought to ride in the underlying asthenosphere. The density is related to the temperature through a constant that is characteristic of the material called the coefficient of volumetric thermal expansion, α_v. For mantle materials this is roughly 3×10^{-5} per degree centigrade, meaning that for every 1 °C drop in temperature the volume

Box 3.2 The cheese sandwich

While in geological problems it is worth committing to memory the rule of thumb that Earth materials have a thermal diffusivity of about 1 mm^2/s, consider the following experiment for determining the thermal diffusivity of another common substance. When we grill a cheese sandwich, we are counting on conduction of heat to allow a thermal wave to propagate through the bread and into the cheese. The sandwich is "done" when the cheese has obtained a particular temperature, namely that of its melting point. This will be some fairly large fraction of the temperature of the base of the skillet you are frying this thing in. The cheese is usually thin relative to the bread surrounding it. So the length scale of concern is the thickness of the bread slice. Call it 10 mm. We also know from experience that it usually takes about 5 minutes to do the job. Using the above equation for the timescale, setting this to 300 seconds, and plugging in 10 mm for the length scale, we find that the diffusivity of bread is about 0.3 mm^2/s. More to the point, especially if you tend to be prone to culinary impatience, you can see how much faster you would be sitting down to eat if you used thinner bread. Sawing off a pair of 7 mm slices instead of 10 mm slices will save you $7^2/10^2$ or roughly 50% in cooking time. Now think about how much time and energy you would save by dicing up that potato you are trying to boil!

decreases by 3×10^{-2} of the original volume. Expressed mathematically, this is

$$\frac{V}{V_o} = 1 + \alpha_v \Delta T \tag{3.9}$$

Consider a chunk of mantle material of given mass, m, and initial density, ρ_o, at a particular temperature. The new density associated with a different temperature is therefore the same mass divided by its new volume. The ratio of the final to the initial density is

$$\frac{\rho}{\rho_o} = \frac{1}{1 + \alpha_v \Delta T} \tag{3.10}$$

We can calculate the density once we know the temperature change to which the material has been subjected. Consider the thermal profile through the lithosphere. At the top of the lithosphere the temperature is that of the ocean floor (about 4 °C), and by definition the temperature at the base is roughly 1200 °C. The thermal profile has a slight curvature throughout, as in Figure 3.4,) so that any parcel of lithosphere continues to cool through time. But to first order the profile is about linear, meaning that the mean temperature in the lithosphere is roughly (1200–0)/2, or 600 °C. The mean temperature of the column of material has therefore declined by 1200–600 or 600 °C. The resulting density change is simply calculated from the above equation to be about + 2% (i.e., $\rho/\rho_o = 1.02$). We can now perform a column balance on two columns, one at the ridge, the other some distance $x(= (u/2)T)$ away from the ridge, as shown in Figure 3.5. We want to know if this can explain, quantitatively, the differing depths of water over the two columns. The ridge top is at a water depth D_o. The other column is under a water depth of $D_o + D$. We want to know how the additional water depth, D, is related to the lithospheric thickness of the column, L. The balance, shown in the figure, results in a ratio of additional ocean depth to lithospheric thickness of roughly 2%. This is very close to the measured relationship.

To summarize, the lithosphere thickens at a rate proportional to the square root of time. The mean density of the oceanic lithosphere is roughly 2% greater than that of the surrounding hotter mantle, and this mean density is approximately the same from place to place. The depth of the droop of the denser lithosphere into the underlying mantle asthenosphere, and hence the depth of the ocean away from the ridge, is therefore controlled solely by the thickness of the lithosphere, and therefore increases as the square root of distance from the ridge. This is in full accord with the observed relationship, which, recall, we determined to be well fit by a square root relationship. We emphasize that the important factor setting the gross topography of the ocean floor is the thickness of the lithosphere and not its temperature. The *mean* temperature of the lithosphere is everywhere the same, as we have defined it by an isotherm on the base, and the top is held at the temperature of the deep ocean, but the thickness of the lithosphere is dictated by the slow downward propagation of the 1200 °C isotherm.

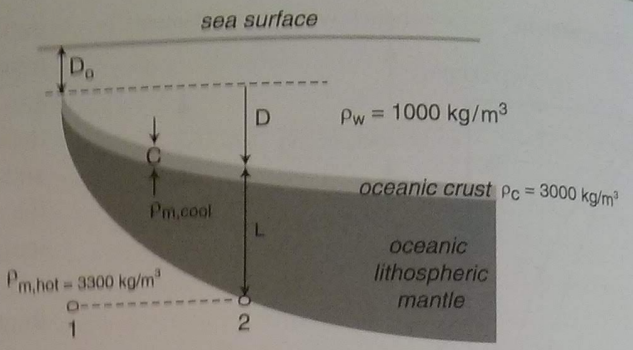

$$\rho_w D_o g + \rho_{m,hot}(D + L)g = \rho_w D_o g + \rho_w D g + \rho_{m,cool} L g$$
$$\rho_{m,hot} D + \rho_{m,hot} L = \rho_{m,cool} L + \rho_w D$$
$$D/L = (\rho_{m,cool} - \rho_{m,hot})/(\rho_{m,hot} - \rho_w)$$

Figure 3.5 Schematic of cooling oceanic lithosphere. Crust achieves and then maintains a 5 km thickness, while lithosphere continues to thicken with time and hence with distance from the spreading center. Depth of the ocean is dictated by isostatic balance: pressures at points 1 and 2 must be equal. Note very large vertical exaggeration.

There are a few interesting wrinkles in this story. As noted when inspecting the bathymetric data, there are systematic departures of the data from this simple square root relation (recall the pattern in Figure 3.2). In particular, both very close to the ridge and very far from it the relation does not appear to describe the full data set. This has prompted considerable research, as departures from simple theories ought to do. The near-ridge anomaly has been attributed to the action of another heat flow mechanism that cools the lithosphere more rapidly than could conduction. The high thermal gradients can drive hydrothermal convection cells within the crust and thin overlying sediment near the ridge, which are very efficient at moving heat about. At greater distance from the ridge, the gradients driving hydrothermal convection diminish, and

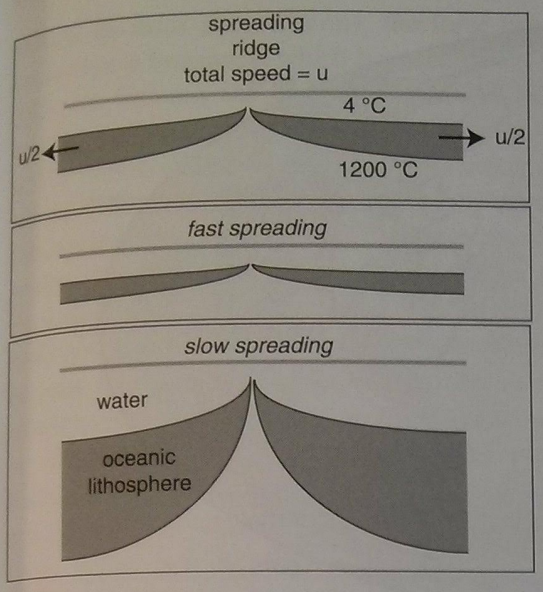

Figure 3.6 Schematic illustration of the role of spreading rate on the bathymetry of an ocean basin. Slow spreading results in a deeper oceanic basin at the same distance from the spreading center, a corollary to the dependence of lithospheric thickness on age.

a layer of sediment acts to seal the fracture permeability of the sea floor, leaving only conduction to perform the task of removing heat from the lithosphere. At very great distances from the ridge (lithospheric ages of more than 80 Ma) it is thought that there might be other sources of heat at the base of the lithosphere, perhaps associated with straining of the underlying mantle materials.

Let us now ponder some large-scale geologic consequences of this model. Consider the age structure of the sea floor. It is straightforward to see that the distribution of ages results in a distribution of ocean depths using the simple model of square root age dependence described above and knowledge of the spreading rates. The present mean age of the oceanic lithosphere is 60 Ma. Note that in the Phanerozoic there is thought to have been little change in the total volume of sea water (save the 150 m-worth that is occasionally sequestered on land in huge ice sheets ... but we shall talk about that later). This means that if we change the mean depth of the ocean floor, and in particular if we diminish it, we will force this water out over the continents, as shown in Figure 3.6. Although there is some current debate about this, some think that this happened in the Cretaceous. The age distribution of the sea floor can be changed by swallowing a spreading ridge, for instance at a subduction zone, or by increasing the speed of ocean spreading at all or some of the ridges. If the mean ocean depth changes by only a few hundred meters, large portions of continents will be submerged. (Remember, the mean freeboard of the continents, including the Tibetan Plateau and other such high places, is only 800 m!) In this hypothesis, faster mean seafloor spreading rates could be responsible for the generation of the huge mid-Cretaceous seaway in the center of the North American continent (Heller *et al.*, 1996), which was itself so important in generating the massive coal deposits along the shores of the western USA. There are other ideas, for example, the thought that the lithosphere is pulled down by the sinking Farallon plate beneath the center of North America, but we will touch upon them later.

Note that we have not dealt here, nor will we deal elsewhere, with the shorter wavelength topography of the ocean basins. This includes seamounts, the abyssal hills (themselves of great interest lately), transform ridges, etc. Two larger scale features bear mention, however. The first are the continental shelves. As one can see from the hypsometric curve, and from the bathymetry of any continental margin, these shelves are confined to water depths of about 0–150 m. They range in width from essentially non-existent on some actively subducting margins, to more than 100 km on passive margins. This raises the question of what controls the width, and why the 150 m maximum depth? It is at least intriguing that the scale of swing of the sea level within the Pleistocene is about 150 m. Highstands, such as the present one associated with low global ice volume, alternate with lowstands as low as 150 m that are associated with large glacial maxima. The latest of these was only 20 thousand years ago. Another aspect of the shelves is that they are in places dissected by very impressive submarine canyons that are at least as deep as the Grand Canyon. The origins of these canyons, when they are active, and what the processes are that etch them into bedrock, remain actively debated and studied problems.

A second major feature of ocean basins is the many chains of volcanic mountains that reflect the passage of a hot spot. At least as interesting as the volcanic mountains themselves are the broad topographic swells that they ornament. We will treat these in the next chapter when discussing flexural support of loads.

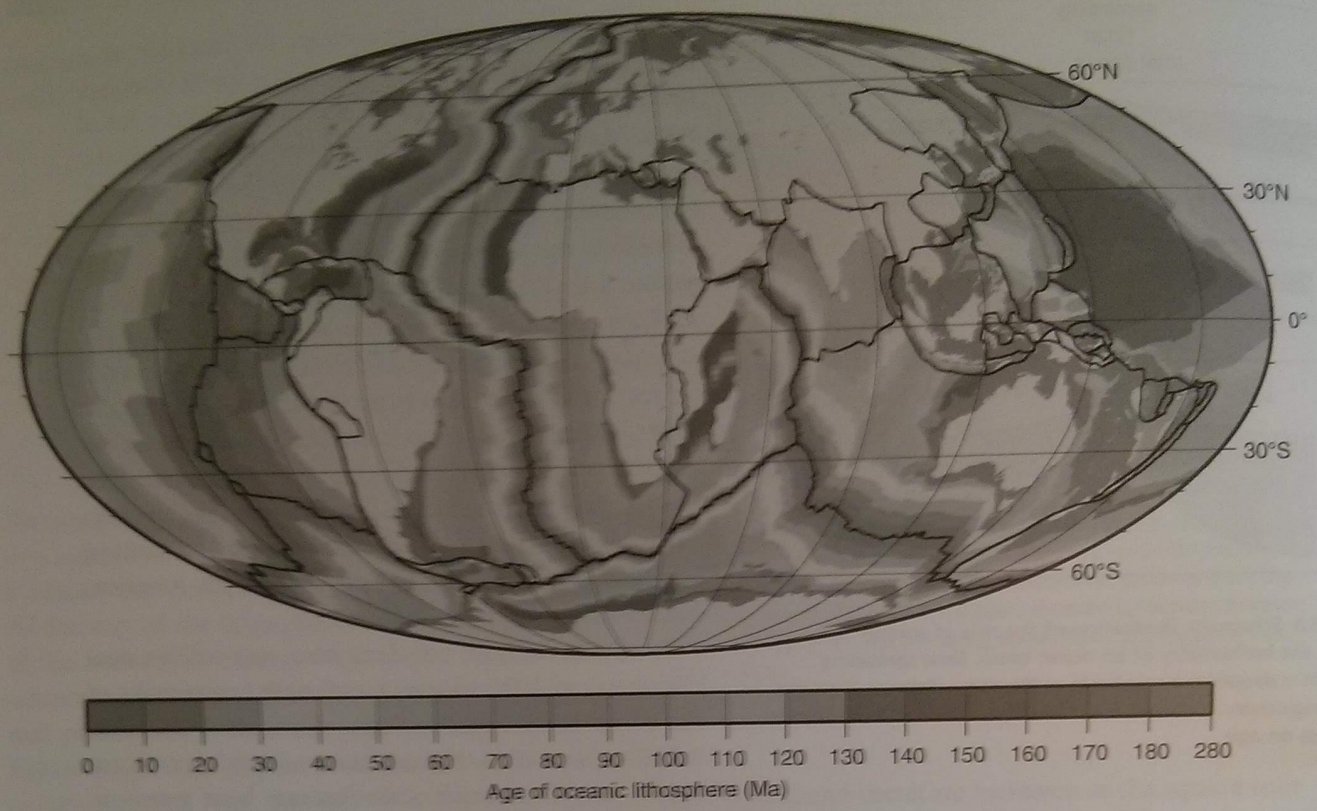

Figure 3.7 Lithospheric plates in their present configuration, with age of oceanic lithosphere. Continents are light gray, shelves dark gray (after Müller *et al.*, 2008, Figure 1a, with permission from American Geophysical Union).

Plate tectonics overview

In this brief overview we lay out first the basic kinematics of plate tectonics (where the plates are, how fast they move, and so on), then turn to a conceptual picture of how this system works, and end with a simple yet illuminating calculation of what sets the speed of plate motion. The major lithospheric plates of the present globe are shown in Figure 3.7. Most are many thousand kilometers in horizontal extent. The plate speeds vary, but most are of the order of 5–15 cm/yr, as can be deduced from the ages of the seafloor.

The motion of plates

The motion of lithospheric plates in plate tectonics is a manifestation of the convection of the Earth's mantle. This outer half of the planet is being both cooled from above, and heated from below. Just as a pot of soup heated from below will ultimately convect, moving hot soup up from below and cold soup from the surface downward, so too will a body of rock heated and cooled under the proper conditions. Likewise, just as a lake cooled from above in the fall and winter will ultimately "turn over," moving cold surface water down to the bottom, so too will the mantle. Both bottom-up and top-down forcing can drive convection. The cooling occurs ultimately through radiation of heat to outer space, and is dictated essentially by the great difference in temperature between the Earth's surface and outer space. The heating at the base of the mantle is caused by its contact with the very rapidly convecting liquid iron of the outer core. Heat moves into the mantle from the core by conduction; it is lost from the mantle to the atmosphere and the ocean by conduction through the lithosphere. The regions within which conduction reigns as the heat transport mechanism are called conductive boundary layers. They are each of the order of a few tens to 100 km thick; the energy transport in the remaining part of the 2900 km-thick mantle is dominated not by conduction but by convection.

Convection can occur whenever the forces driving overturn of a fluid are greater than those resisting such

motion. In most general terms, the force promoting convection is buoyancy, which is scaled by the density difference between the one portion of the fluid and another, and by how big this blob of anomalous fluid is. The density difference can arise from either compositional or thermal effects; in the case of mantle convection, thermal effects dominate. The force resisting this motion scales with the viscosity of the fluid, and with the surface area of the anomalous blob. It is common to derive a ratio of driving to resisting forces that may be used to characterize whether or not convection should occur, and how vigorous the convection might be. This ratio, which is dimensionless, is called the Rayleigh number, denoted Ra, and is one of many non-dimensional numbers we will encounter in this book. When this Rayleigh number is above about 2000, convection driven by thermal buoyancy should occur. For the Earth's mantle, the Rayleigh number is presently of the order of 10^5, meaning that it ought to be convecting quite vigorously.

Plate speeds

Given this physics, how fast ought plates to be moving in the Earth mantle system? Can we, from first principles, predict the rates at which the plates are moving about on the Earth's surface? Given that plate tectonic movement rates determine the pace of mountain building events, which drive rock above sea level where terrestrial erosive surface processes can attack it, and generate topographic gradients that dictate the rates of geomorphic processes, this is a crucial number. In addition, note that if we have a theory that allows calculation of these rates, we will be in a position to evaluate quantitatively how these rates might have been different in the past, when the Earth was younger and perhaps even more vigorously convecting.

The problem may be reduced to a force balance. If we assume that the plates are not accelerating, in other words that they are moving at the same rate today as they were last year as they were hundreds of years ago, which is probably a safe assumption, then the forces that are driving them must be in balance. This is a simple restatement of Newton's second law: $F = ma$, where F is the sum of the forces operating to cause motion, m is the mass of the object, and a is the acceleration. The object of concern is a lithospheric plate. We simply have to identify the forces acting on

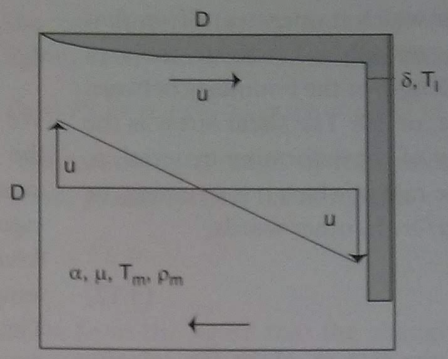

Figure 3.8 Sketch of mantle "convection in a box" of width and depth D at a rate u. Lithosphere (gray) thickens to δ at time of subduction. Balance of negative buoyant force driving convection, and viscous drag resisting it, yields an estimate of the speed of convection, u (see text for details) (redrawn from Davies, 1999, Figure 8.1, with permission from Cambridge University Press).

the plate, and equate them, as shown in Figure 3.8. The problem is akin to a settling problem with which we are more familiar, and which we will turn to in discussing sediment transport in fluids, except that the object that is settling is not a sphere, but a slab. The forces operating are F_b, the (negative, downward) buoyant force of the slab, caused by its having a density that is slightly higher than the remainder of the mantle, and F_r, the (positive, upward) resisting force, caused by viscous drag along the surface of the slab as it descends through the very viscous mantle. Our task is to estimate the magnitude of each of these terms and set them equal (so that their vector sum is zero). First, we need an equation for the buoyancy force. Let's consider a unit thickness of mantle (into the page), in which case we need expressions for the force per unit width. If the thickness of the mantle is D, and the width of the convecting cell is also D (a crude approximation), then the buoyant force per unit width of slab pulling it downward is

$$F_b = D\delta g(\rho_l - \rho_m) \tag{3.11}$$

where δ is the thickness of the lithosphere upon subduction, g is the acceleration due to gravity, and ρ_l and ρ_m are the lithospheric and mantle densities, respectively. The force increases linearly with the thickness of the slab upon subduction.

The resisting force is a drag force, or a surface traction, that operates on the surfaces of the slab. This requires knowledge of the shear stress (a force per unit

area) and the area over which it operates. Given that we are doing a balance on only a 1 m sliver, the area really translates to the length of the boundary between mantle and lithosphere, or $2D$. The shear stress is the product of the viscosity of the deforming material, μ, here the mantle, and the rate at which it is straining, or the shear strain rate, $\partial u/\partial r$. In other words,

$$F_v = 2D\tau = 2D\mu\frac{\partial u}{\partial r} \tag{3.12}$$

Here the shear rate is the rate at which the velocity within the mantle changes with distance away from the lithosphere (see Figure 3.8). Using knowledge that the whole mantle cell is turning over with a speed of u at its perimeter, meaning that while the right-hand side is going down at u, the left-hand side is coming up at $-u$. The difference, $2u$, occurs over a distance of D, meaning that $\partial u/\partial r = 2u/D$. Equating the buoyant driving and the resisting forces per unit length, and solving for the unknown velocity, results in

$$u = \frac{D\delta g(\rho_l - \rho_m)}{4\mu} \tag{3.13}$$

The thicker and longer the lithospheric slab, δ, the faster it will settle into the mantle, while the higher the viscosity the lower its speed will be. It remains to calculate the thickness of the lithosphere, and the density difference between lithosphere and mantle. The lithosphere thickens by conduction (as we have discussed above), which is controlled by the thermal diffusivity, κ, and the time since cooling at the surface began. In particular, $\delta = \sqrt{kT} = \sqrt{k(D/u)}$, where T is the time it takes for the lithosphere to move from spreading center to subduction zone. Note that the faster the mantle turnover rate, the thinner the lithosphere will be by the time it subducts. We have also discussed the density difference between lithosphere and mantle, as we needed this number in order to evaluate the isostatic balance. The density difference is simply

$$\Delta\rho = \alpha\Delta T\rho_m \tag{3.14}$$

where ΔT is the difference in temperature between the lithosphere and the surrounding mantle. This leaves us with the following equation for the speed of the plate:

$$u = \frac{Dg\alpha\Delta T\rho_m\sqrt{\kappa D/u}}{4\mu} \tag{3.15}$$

or, noting that u is involved in the thickness of the lithosphere,

$$u = \left(\frac{Dg\alpha\Delta T\rho_m\sqrt{\kappa D}}{4\mu}\right)^{2/3} \tag{3.16}$$

We now need to estimate all of these variables. What is the temperature difference between mean mantle and mean lithosphere? Given that the surrounding mantle is vigorously convecting and hence does not vary greatly from that at the base of the lithosphere, we can take its temperature to be that of the base of the lithosphere. The mean temperature of the lithosphere is well approximated by the average of its top and its base, given that the thermal profile within the lithosphere is crudely linear. Hence, $\Delta T = 1200 - ((1200 - 0)/2) = 600\,^{\circ}\mathrm{C}$. The other variables may be taken to be: $D = 2900\,\mathrm{km} = 2.9\times10^6\,\mathrm{m}$, $g = 10\,\mathrm{m^2/s}$, $\rho_m = 3.3\times10^3\,\mathrm{kg/m^3}$, $\kappa = 1\,\mathrm{mm^2/s} = 10^{-6}\,\mathrm{m^2/s}$, $\mu = 10^{21}$ Pa-s, and $\alpha = 3\times10^{-5}/^{\circ}\mathrm{C}$. The resulting estimate of plate speed (really the half-spreading rate) is 3.6×10^{-9} m/s, or 0.11 m/yr. We have already documented actual plate speeds, which are a little slower than this, typical convergence rates being more like 5–10 cm/yr, and hence 2.5–5 cm/yr for expected half-spreading rates. Nonetheless, given the approximations made in setting up the problem, and the necessarily crude estimates of the values of the parameters, we have come astonishingly close to reality!

It is also instructive, before we leave this calculation, to inspect the final equation for the velocity, and assess how this might have changed through geologic time. Among all these variables, what is likely to have changed? Physical constants like g and α and κ certainly will not have changed. The variable that is most susceptible to change is the viscosity of the mantle. Viscosity is a temperature-dependent property of a material. In particular, it declines greatly with increasing temperature, exponentially so. If the mantle in early times were significantly warmer than it is now, then the viscosity would have been much lower. Note that $u \sim \mu^{-2/3}$. If the viscosity were an order of magnitude (ten times) lower in the early Earth, then the plate speed would have been $(1/10)^{-2/3}$ or 4.6-fold faster then. It is a good thought experiment to explore the implications of this for the topography of the early Earth.

Large-scale mountain ranges: orogens

The support of the world's largest mountain ranges is similar to that of the ocean basins. Isostasy

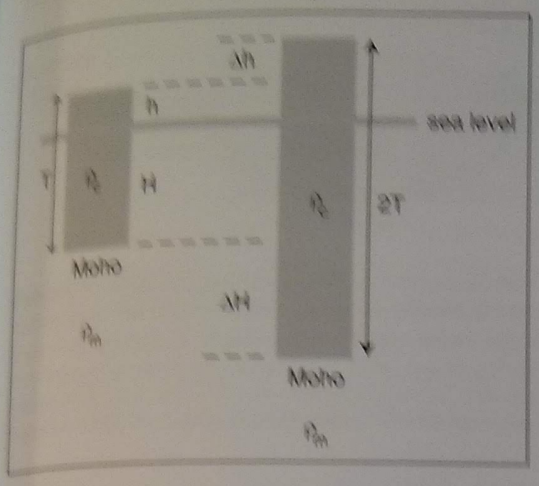

Figure 3.9 Isostatic response to doubling of the crustal thickness. Deepening of the Moho greatly exceeds the increase in the freeboard of the continent (its height above sea level).

reigns. The support of the topography is largely through buoyancy. The topography reflects the thickness of low-density crustal material beneath it. In this section we will explore the geophysical consequences of erosion on a large scale, and explore issues related to the response of continental land-masses to the thickening of the crust, taking the Tibetan Plateau as our example. We will ask the questions: how does the elevation of a mountain range respond to the removal of material from the range by erosion? Does the pattern in which the material is removed play a role? We will see that we need to be careful in exactly how we pose the questions, and where within the landscape one might seek the answers to the questions.

Effects of thickening the crust

In Figure 3.9 we show a column of continental crustal material of thickness T, in isostatic balance such that it floats with a mean elevation of height h above sea level, and a depth to the Moho of H below sea level. If by some mechanism the crustal material were greatly thickened, say doubled, by how much would the mean elevation of the range and the mean depth to the Moho change? The problem is perfectly analogous to exploring the change in freeboard of a slab of ice if you place another slab on top of the first. The pressure at an arbitrary depth within the mantle beneath the base of the crust must be the same in the two cases, allowing us to set P_1 and P_2 equal again, as in our previous column balances:

$$P_1 = P_2 \Rightarrow \rho_c T g + \rho_m \Delta H g = \rho_c (2T) g \tag{3.17}$$

Again dividing through by the gravitational acceleration, g, and solving for ΔH yields

$$\Delta H = \frac{\rho_c}{\rho_m} T \tag{3.18}$$

Note from the figure that the change in mean elevation, Δh, is simply obtained from $2T = \Delta h + T + \Delta H$. Using our expression for ΔH, we arrive at the expression for the change in mean elevation:

$$\Delta h = T - \Delta H = T\left[1 - \frac{\rho_c}{\rho_m}\right] \tag{3.19}$$

Given typical values for densities of crustal and mantle material, of 2700 and 3300 kg/m^3, respectively, the term in the brackets becomes 2/11, or roughly 20%. If no erosion were to occur during the thickening of the crust, doubling of the crust would drive a change of elevation of roughly 20% of the change in crustal thickness, while the rest, or 80%, results in lowering of the Moho.

Let's explore an example. The Tibetan Plateau in central Asia has resulted from the collision of India with Asia, a collision that began roughly 40 Ma, and continues today at plate convergence rates of about 6 cm/yr. This is the world's greatest example of continent–continent collision, and results in the largest welt of high topography (Figure 3.10). Mean elevations of the plateau are close to 5 km over a 1200 km N–S transect. Let's work in the reference frame of Asia. Sitting on Asia, it looks like the Indian subcontinent, with its continental crust of thickness T, is arriving at the plate boundary at a rate u. What happens at depth at this boundary is hotly debated. But it appears that a large fraction of the Indian continental crust is somehow tucked underneath the Asian continental crust. If the crusts of the two continents were roughly 25 km thick to begin with, this would result in a 50 km-thick crust beneath the Plateau. The change in thickness of 25 km should result in a change in elevation of roughly 2/11 of 25, or roughly 5 km. This is remarkably close to the mean elevation of the Plateau, supporting the notion that the crust has been roughly doubled.

Can this explain the width of the Plateau as well? We wish to craft a volume balance on the crustal

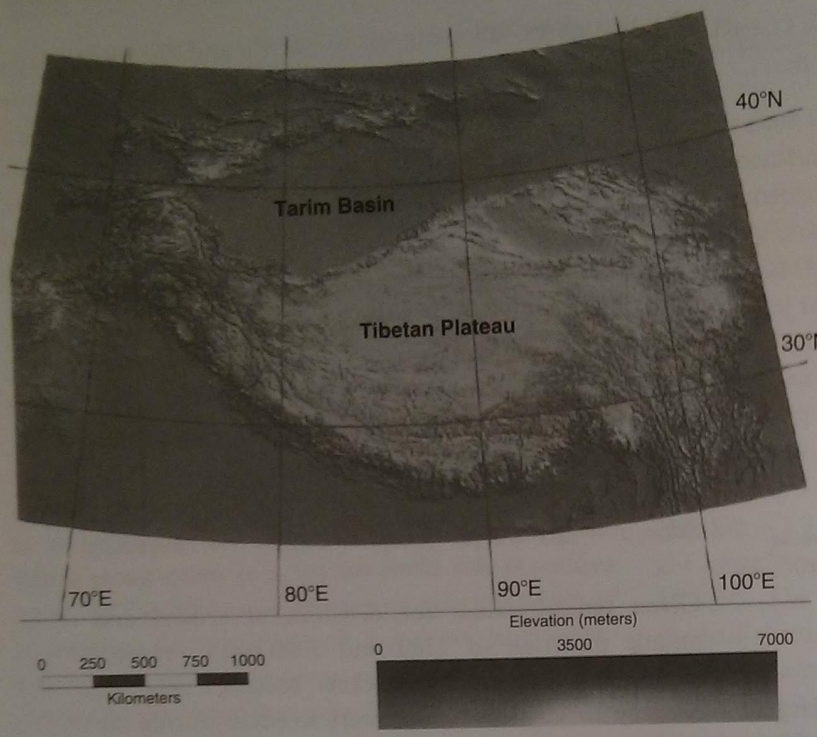

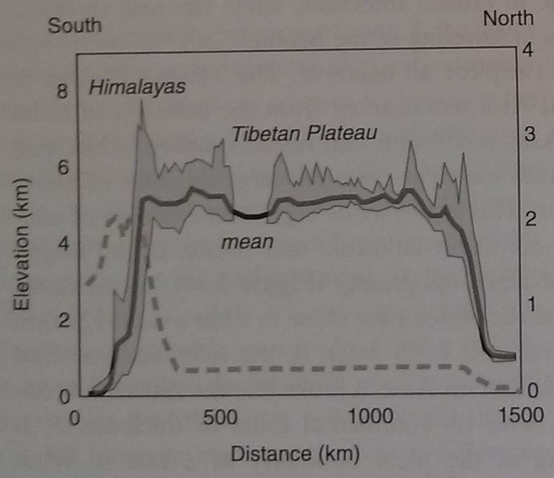

Figure 3.10 (a) Topography of Tibet using SRTM 90 m data. (b) N–S topographic swath profile across the plateau. Gray shaded band encloses all topography; black line is the mean topography in the 100 km-wide swath. Note the abrupt edges and the flat top of the plateau, with mean elevation ~5 km. The precipitation profile (dashed) illustrates the strong orographic effect: precipitation is effectively milked from the clouds as they encounter the Himalayan front from the south. Highest relief is at the edges of the plateau, most impressively at the southern edge in the Himalayas (after Fielding *et al.*, 1994, Figures 2 and 3).

material, depicted in Figure 3.11. (Actually, this is a cross-sectional area balance.) If the entire Indian continental crust has been tucked beneath the Plateau, then the total cross-sectional area of crust ought to be the original thickness T times the width W, plus that contributed since the collision. The crust added since collision is simply the thickness of Indian continental crust, T, times the rate at which it is arriving at the plate boundary, u, times the total time since collision began, t. The measured depth to the Moho is roughly 50 km, or $2T$. Setting the measured cross-sectional area $2TW$ equal to the original TW plus the newly arrived crust Tut, results in an expected width $W = ut$. Given the convergence rate of 6 cm/yr $= 6\times10^{-5}$ km/yr and a time since collision of 40 Ma $= 40\times10^{6}$ years, we predict the width of the plateau to be 2400 km – too wide by almost a factor of two. The error could be due to any of several assumptions we have made: the thickness of Indian crust could be less than that of Asia; the plate rate we have used might not be representative of the mean rate since 40 Ma; the time of collision could be more recent; or

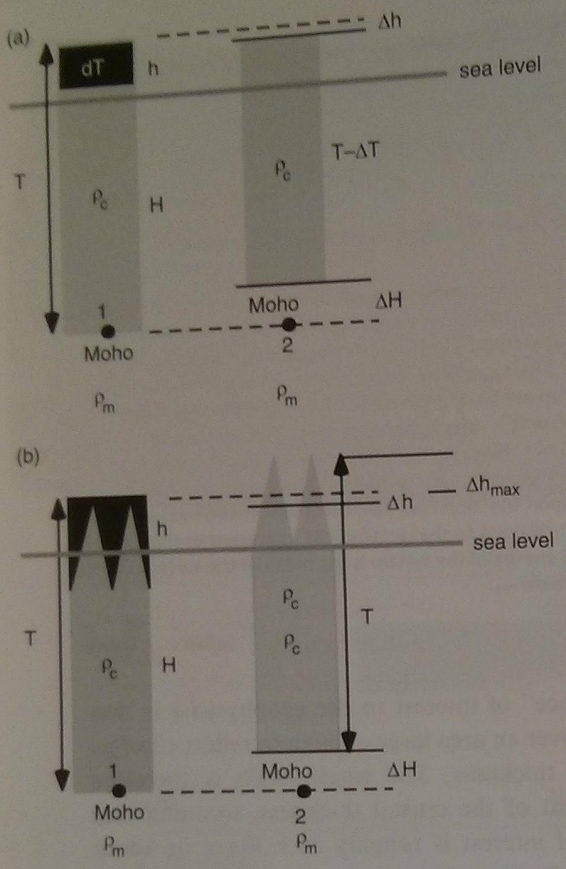

Figure 3.13 Effects of non-uniform erosion on peak elevation. While mean elevation declines due to removal of crustal mass, the greater erosion in valleys during times of increasing relief can result in the uplift of peaks (adapted from Molnar and England 1990, Figure 2, with permission from *Nature*).

crude geometry of the triangular valleys we have chopped into the crustal block, or $0.9h$. Note that no matter whether we are eroding uniformly or non-uniformly, the mean elevation of a range declines during erosion – by a small fraction of the mean thickness removed, but a decline nonetheless.

The possibility of raising the elevations of peaks within a range by simply deepening the valleys within it, enhancing the relief of the range, is intriguing. As again noted by Molnar and England in their provocative paper, this linkage can set up some interesting feedbacks in the climate–topography–geomorphology–isostasy system. As we will see in our discussion of glaciers, the health of a glacier (called its mass balance) depends upon how much of the mountain valley within which it exists lies above the snowline, an elevation (the equilibrium line altitude, or ELA) above which some of a winter's snow remains unmelted at the end of the next summer. The higher a mountain mass, the more healthy the glacier. If in addition, the glaciers, which occupy the valleys of the range, are efficient erosional agents, as we will see they are, then the possibility exists that further erosion of the valleys makes the glaciers more healthy, further deepening the valleys, and so on. A positive feedback loop has been established.

Another feedback has to do with precipitation as it interacts with a mountain mass. Local precipitation is milked out of an air parcel as it is forced to rise over a mountain range in something we call an orographic effect (oro- for mountain related, like orogeny). On a local scale, the air mass does not care about the mean elevation of a range, but instead must go over the peaks in the range. So peak elevations matter to the atmosphere. The higher they get, the more precipitation will be milked from the clouds locally on the windward side of the range, leaving less for the downwind side. This orographic effect implies that relief production within a range might intensify rain shadows in the lee of a range. Let us explore a couple of examples.

The Tibetan Plateau again serves as an example. Note that the south side of the Plateau is bounded by the huge Himalayan chain of mountains, with many of the world's 8000 m peaks. As shown in the cross section of the topography in Figure 3.10, compiled from a large digital elevation data set, the mean elevation of the Himalayas is roughly that of the Tibetan Plateau. In contrast, the relief (the differences between highs and lows in the topography) of the Plateau is minuscule in comparison to that within the Himalayas. Note the pattern of precipitation rates. The precipitation arrives at the Himalayas from the south, delivered by the Asian monsoon from the Indian Ocean. Tibet is extremely dry, living in the rain shadow of the Himalayas. To first order, we can think of the Himalayas as simply an eroding edge of the plateau. The non-uniformity of this erosion, resulting from efficient rivers and glaciers, has generated huge valleys, and high relief. The isostatic response to this relief production has raised the highest of the peaks to roughly 1.8 times the mean height of the low-relief plateau, or 8000 m.

Many questions remain in this landscape. When within the collision was this relief produced? Has it always been there? Has the global cooling in the late Cenozoic produced glaciers, which in turn have generated relief, producing rock uplift? There exists a

strong possibility of misinterpretation of the rock record, as again pointed out by Molnar and England (1990), and their principal motivation for the paper. Is it a pulse of tectonics in the late Cenozoic that raised the Himalayas and produced a pulse of sediment from the mountains, or was it climate change? (That both can lead to a pulse of sedimentation in basins that bound ranges makes the interpretation of such basin sediments ambiguous – leading to the title of their paper asking whether it is the chicken or the egg.) Another potential consequence of the raising of Tibet is the aridification of central Asia. At present, the monsoon rains are trapped at the leading edge of the plateau, the Himalayas, and cannot penetrate into the interior (see the precipitation pattern in cross section of the plateau in Figure 3.10). One of the key attributes of central Asia is its deserts, the Gobi, the Taklamakan, and so on. Downwind of these, throughout what is now China, is the most extensive deposit of dust in the world, the Loess Plateau, with loess thicknesses of hundreds of meters. The age of the base of the loess deposit is roughly 8 Ma, which corresponds well with the age of the inception of the monsoon as deduced from paleo-oceanographic records in the Arabian Sea. Perhaps the two events are linked: the growth of the Tibetan plateau triggers the monsoonal pattern of precipitation, which in turn aridifies the region downwind of the plateau.

Mantle response times: geomorphology as a probe of mantle rheology

We now ask what determines the timescales of response to the emplacement or removal of crustal loads. Formally, the elastic response is essentially instantaneous, traveling at the speed of sound within the material. Stand on a diving board and it responds immediately; jump off from it and it rebounds instantly to its old position. The fluid response, however, which becomes increasingly important as the scale of the load increases (as the degree of compensation C increases toward 1.0), is dictated by the time it takes for the deep crustal or upper mantle material to move out of the way of a new load in response to the pressure gradients established by that load. This timescale is determined by the viscosity of the fluid, and hence serves as a probe of the mantle viscosity. The higher the viscosity, the longer it takes to respond to an applied load. For mantle materials, the timescale is of the order of several thousand years. Importantly, we know this timescale largely from the deflection of datable geomorphic markers in the landscape. The large-scale ice sheets and lakes that have relatively recently met their demise constitute natural experiments that provide us with major constraints on mantle viscosity. The wavelength of the load has to have been large enough (of the order of several hundred kilometers) to involve the buoyant response in order to allow the load to serve as a probe of mantle viscosity. The longer the wavelength of the load, the greater the volume of mantle is involved in the response to the loading; larger loads are therefore better probes of deeper mantle viscosity structure.

The first discussion of the use of this sort of geomorphic deep-Earth probe can be found in G. K. Gilbert's (1890) classic monograph on Lake Bonneville (the first USGS monograph). Gilbert used the variation in the heights of shorelines that were all formed in a very short period of time, called the Bonneville shoreline, to map the deflection field associated with the Bonneville Lake load. Lake Bonneville flooded the eastern portion of the Basin and range province, which is studded with north–south trending mountain ranges bounded by normal faults. Because each of these ranges has shorelines corresponding to the Bonneville highstand, Gilbert was able to map the subsequent deflection of the shorelines simply by noting their elevations. The resulting map reproduced in Figure 3.14 looks like a bulls eye, with a maximum upward deflection of the shorelines of over 50 m. We now know from ^{14}C dating that the Bonneville shoreline was formed about 14.5 ka. Of course, at the time it was formed, this shoreline was everywhere the same elevation. That it is now warped up in the center implies that at the time it was formed the load of the lake deflected it downwards by at least this much. Importantly, there are also other younger shorelines that show a pattern of deflection as well. These can be used to document the temporal evolution of the Bonneville area to the removal of the load. It is from the timescale of this response that the viscosity of the upper mantle can be read (see Bills *et al.*, 1994).

Other sites that have been used as probes of mantle behavior include the rebounded shorelines around the edge of Hudson's Bay and in Fennoscandia, reflecting the isostatic rebound from the removal of the Laurentide and Fennoscandian ice sheets, respectively

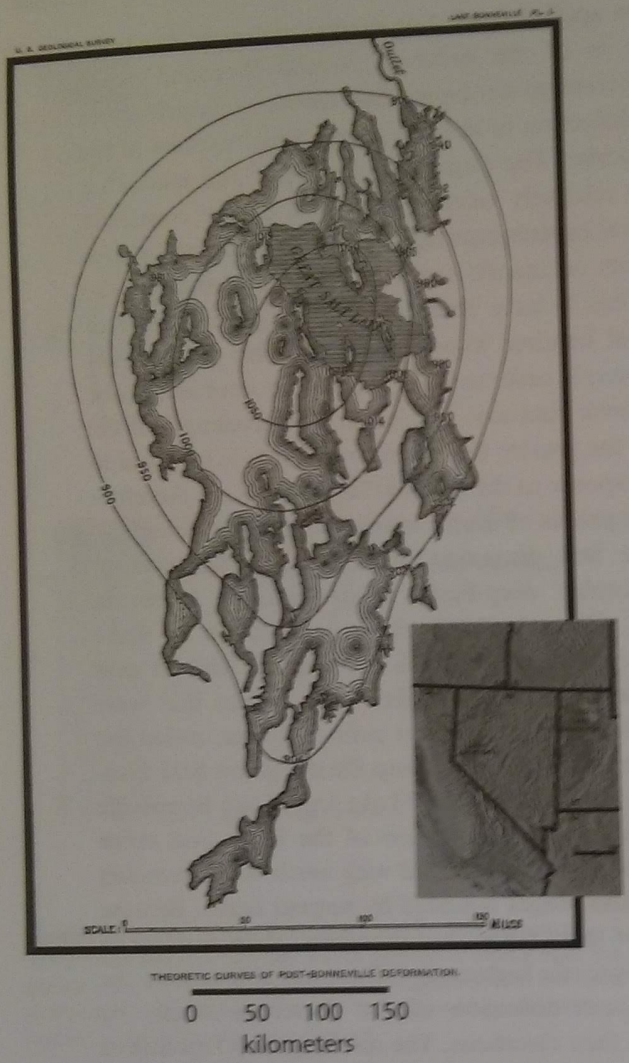

Figure 3.14 Pattern of isostatic rebound associated with loss of Lake Bonneville (G. K. Gilbert, 1890, Plate L). Present remnant of Lake Bonneville is the Great Salt Lake (horizontal lines). Contours of Bonneville shoreline elevations (Gilbert's original is in feet above the Great Salt Lake elevation) show warping of at least 150 ft, or about 46 m.

(e.g., Walcott, 1972; Andrews, 1968; see summaries in Cathles, 1975, and Watts, 2001). Lake Ayre in Australia and Lake Uyuni in the altiplano of the Andes have been used as well.

Ice sheet and ocean loading and the response of the Earth surface to it

We have discussed the load associated with Lake Bonneville. While this is locally important, the volume of water involved is not globally significant. In great contrast, the volume of ice tied up in ice sheets at present and in the past is significant. The sum of the present volumes of ice on Greenland and in Antarctica is worth about 80 m of sea level; if they were to melt, sea level would rise 80 m. And at the last glacial maximum (LGM), enough additional ice was tied up in the great ice sheets covering northern North America and Fennoscandia that sea level was depressed by 120–150 m. In other words, the loading of the northern continents by ice coincided with the unloading of all the world's oceans, and conversely, during deglaciation, the unloading of the northern continents coincided with the reloading of the ocean basins. We illustrate this in Figure 3.15. Here we summarize the response of the Earth's surface to these large-scale changes in the pattern of loading. It is important to acknowledge that the Earth is still responding to these changes, as the timescale for the response, dictated by the mantle viscosity, is a significant fraction of the time since deglaciation. We cannot understand the pattern of the modern rates of relative sea level change, as documented by tide gages, for example, at points along the world's coasts without addressing this component of surface uplift or subsidence. What is clear from both the data and from models of the full mantle response is that the signal of growth and decay of ice loads on the surface of the Earth has incited a truly global response, as seen in Figure 3.15, that must be acknowledged when trying to interpret modern gravity (GRACE), tide gage, tilt, and GPS records. While it is clear that a river like the Mississippi, whose headwaters were covered by the southern margin of the Laurentide ice sheet, will have been directly and greatly affected by the ice loading, it is less clear how a river like the Amazon will have been affected. We will discuss rivers at greater length elsewhere, but it should be intuitive that the larger a river is, the smaller will be its slope. We will see that the broad tilting of the continental margin driven by the loading and unloading of the adjacent ocean basins is of the same scale as the slopes of these large rivers.

Consider the simple representation of a pattern of loading that is triangular, tapering from a peak at the load center to zero at the margin. This is depicted in Figure 3.16. For the moment, imagine that this load is emplaced instantaneously. For our purposes, this means it is placed more rapidly than the underlying mantle can respond. We ask what determines the

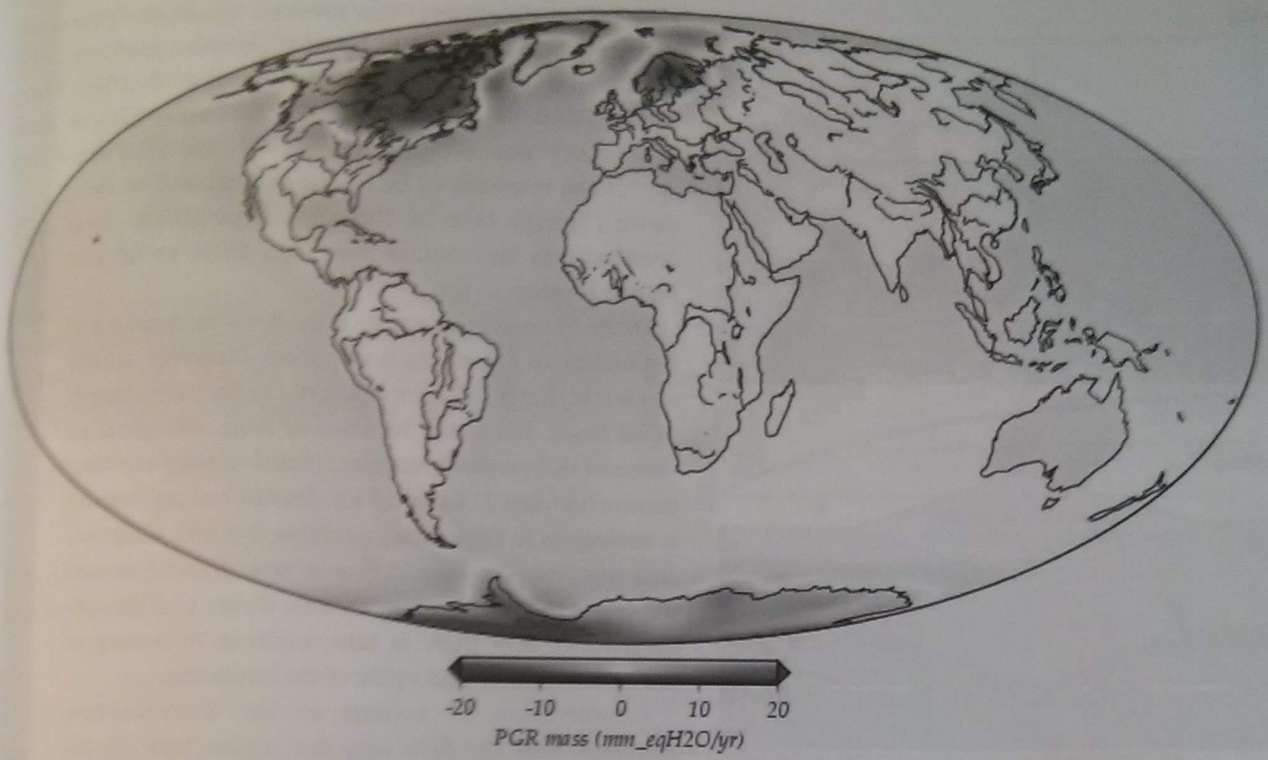

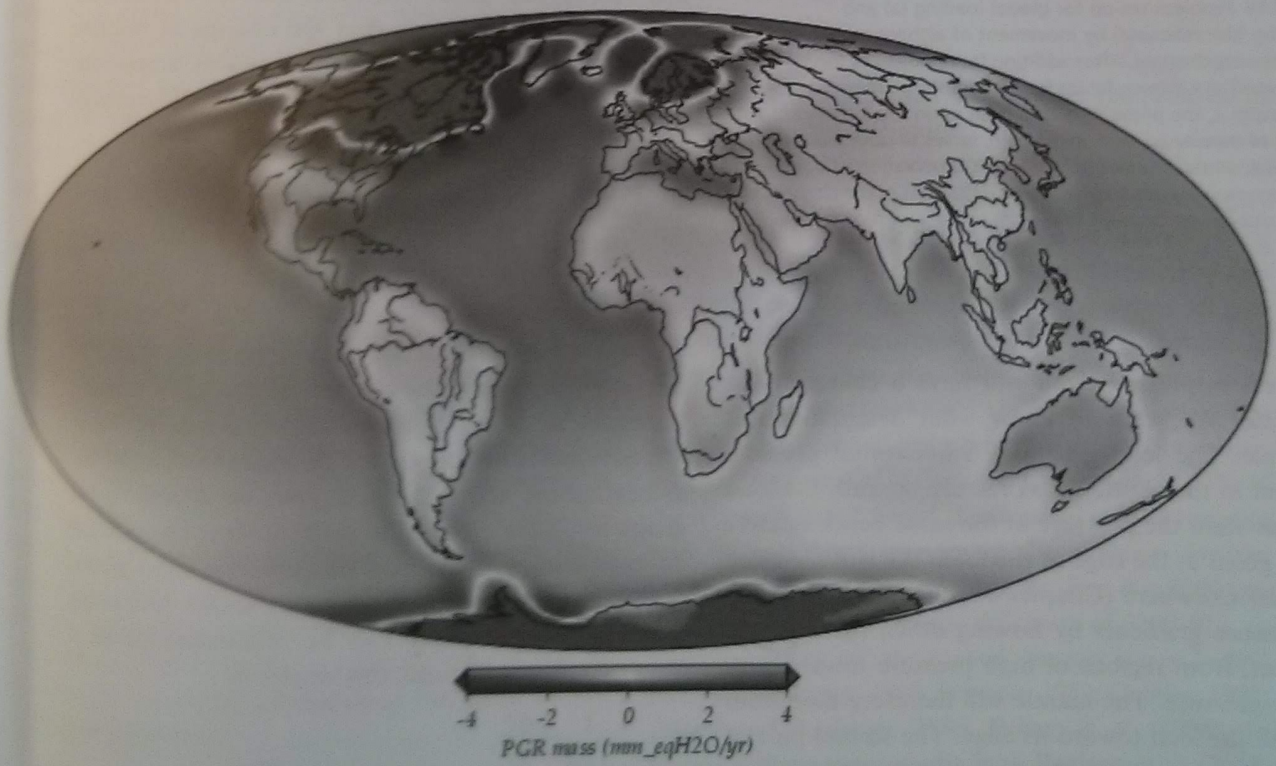

Figure 3.15 Predicted global distribution of post-glacial rebound (PGR), calculated using a prescribed glacial history (ICE-5G from Peltier (2004)), 90 km-thick lithosphere, 1170 km-thick upper mantle with a viscosity of 0.9×10^{21} Pa-s, and lower mantle viscosity of 10×10^{21} Pa-s. Scales reported as surface changes in mm of water equivalent per year. The panels differ only in the color scale. Top: wide range shows details to be seen in the region of large load changes over the ice sheet sites. Bottom: reduced scale allows details to be seen in the remainder of the world far from ice sheet influences. While collapse of the forebulges associated with the ice sheets produces the greatest subsidence rates, the reloading of the ocean basins causes subsidence that is greatest immediately outboard of the continental margins (figure in personal communication from A. Paulson, with permission to reproduce).

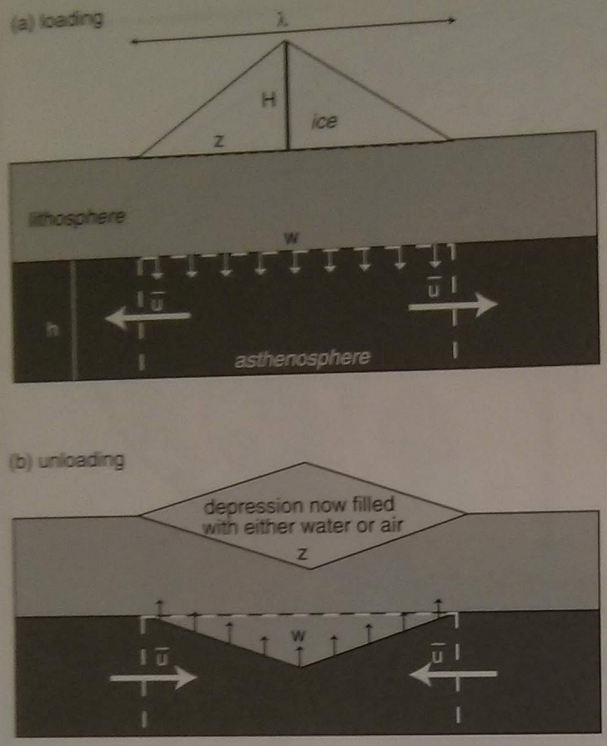

Figure 3.16 Problem set-up for glacial loading (a) and unloading ((b): rebound) by movement of asthenosphere in a low-viscosity channel. After addition (or removal) of the ice sheet, here treated as a triangular ice load of density ρ_i, maximum height H and width λ, the pressure gradient set up in the asthenospheric channel of density ρ_m, and thickness h, serves to push mantle away from (back under) the site of the load. Conservation of volume in the asthenosphere requires deflation (inflation) of the channel at a rate w, and hence decrease (increase) in the elevation of the surface, z.

temporal response, which will have a characteristic timescale. We want to know what determines this timescale. The load generates a horizontal pressure gradient in the mantle; the pressure beneath the load is larger than the pressure at the same depth relative to the geoid at the edge of the load. We will see more formally elsewhere (Chapter 10) that fluids respond to pressure gradients by flowing down the pressure gradient, from regions of high pressure toward sites of low pressure. The mantle will therefore flow from beneath the load toward its edge. The second part of the problem is conservation of mass in the asthenosphere. Loss of mass from asthenosphere beneath the load leads to thinning of the asthenosphere. As the asthenosphere thins, the load settles downward, decreasing the pressure beneath the center of the load, and hence decreasing the pressure gradient. This will continue until the horizontal pressure gradient driving the mantle away declines to zero, at which point in time no more flow can occur. This condition is formally one of isostatic balance. We therefore expect the response to be fastest at first, and to slow down through time as the pressures equalize. You could sketch this out; it is a good habit to do this before turning to the math.

In the discussion above, we considered the response of the surface to loading by an ice sheet. However, we live in a world that is still responding not to the emplacement of ice loads, but to the removal of them. The great ice sheets of the northern continents most recently met their demise between 22 ka and 7 ka. The unloading problem is analogous to the loading problem, but with the gradients reversed: the mantle flow is now directed toward the centers of the now-vanished ice sheets, and the convergence of flow there in turn results in thickening of the asthenosphere and uplift of the landscape.

Conservation of volume in the asthenosphere demands that the flow into the region beneath the load, across the "gates" shown as dashed vertical lines in Figure 3.16, demands that the change in volume between the gates equals the gain or loss across the edges. This results in the equation for the vertical velocity of the surface, w:

$$\lambda w = 2h\bar{u}$$

or

$$w = \frac{2h\bar{u}}{\lambda} \tag{3.20}$$

where λ is the width of the load, $\bar{u}$ the mean speed of the asthenosphere in the channel of thickness h, and z the mean elevation of the surface beneath the load. We now need an equation for the mean velocity of the asthenosphere across the gate. Here we appeal to the geometry of the problem as we have set it up, and use an expression for the flow between two rigid plates (although of course this is a simplification). Assuming that the asthenosphere can be approximated as a linear viscous substance, this results in

$$\bar{u} = -\frac{1}{12\mu} h^2 \frac{dP}{dx} \tag{3.21}$$

The velocity is inversely proportional to the viscosity, and is sensitive to the thickness of the channel. The negative sign assures that the flow moves down the gradient, dP/dx. The final piece of the puzzle is then

the estimation of the horizontal pressure gradient. This is scaled by the difference in pressure at the load center and edge, divided by the distance between these. In the case of unloading, this pressure gradient can be approximated by

$$\frac{dP}{dx} = \frac{P_{edge} - P_{center}}{\lambda/2} = \frac{2\Delta\rho g \Delta z}{\lambda} \tag{3.22}$$

where $\Delta\rho$ corresponds to the density difference between asthenospheric mantle and the infilling material (water or air). We can now assemble these pieces to arrive at a differential equation for the rate of uplift:

$$w = \frac{d(\Delta z)}{dt} = -\frac{h^3 \Delta\rho g}{3\lambda^2 \mu} \Delta z \tag{3.23}$$

This linear first-order ordinary differential equation may be solved to yield

$$w = w_o e^{-\frac{t}{3\mu\lambda^2/\Delta\rho g h^3}} \tag{3.24}$$

This exponential equation conforms to our expectation of a rapid initial response, which then decays through time. Note that the collection of constants in the numerator must have units of a timescale. Indeed, this is the characteristic timescale, τ, for the response of the mantle: $\tau = (3\lambda^2\mu)/(\Delta\rho g h^3)$. The equation may therefore be written more simply as

$$w = w_o e^{-t/\tau} \tag{3.25}$$

The history of uplift rate, $w(t)$, is shown in Figure 3.17. The surface elevation rises rapidly at first and then more slowly through time. The timescale, τ, corresponds to the time it takes for the rate of rise of the surface to decline to (1/e) of its original rate. The lithosphere is therefore still on the move for times of a few times this characteristic time, or several τ. We can see now that the timescale is determined by the mantle viscosity. This calculation lies at the core of the utility of geomorphic markers as probes of mantle viscosity.

By integrating the equation for the rate of rise of the surface, we derive an equation for uplift of the surface through time:

$$\Delta z = \Delta z_o \left[1 - e^{-t/\tau}\right] \tag{3.26}$$

where Δz_o is the expected final deflection of the surface at very long times $t \gg \tau$. This is asymptotically approached at long times, $t \gg \tau$, after the removal of the load, as seen in Figure 3.17.

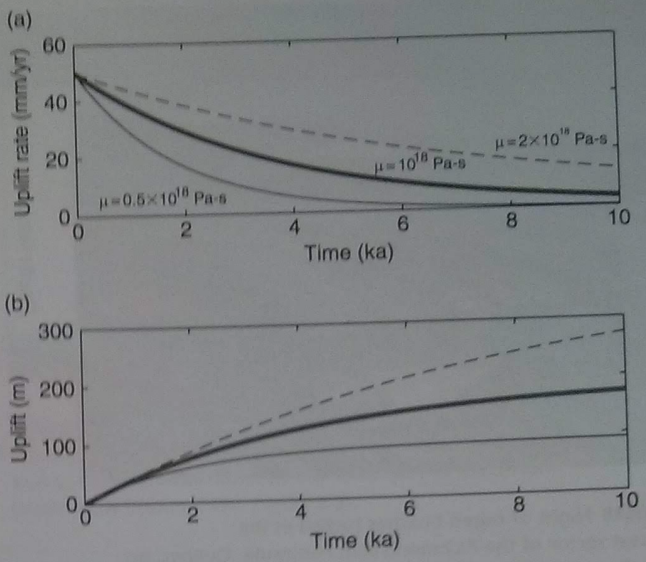

Figure 3.17 Theoretical rebound histories for three mantle viscosities with identical prescribed initial rebound rates. (a) Rebound rate histories displaying different characteristic timescales, shorter times associated with lower viscosities. Asthenospheric channel thickness 200 km, 1000 km-wide load, density contrast between mantle and infilling material = 3300 kg/m^3. (b) Deflection histories obtained by integrating the rebound rate histories.

It has long been recognized that glacial rebound is the cause of the raised beaches in the Hudson Bay area, and in Sweden (Figure 3.18). These beaches can be dated using ^{14}C in shells they contain. These dates and the elevation of the shorelines comprise a data set that has been used to constrain local mantle viscosities. In Figure 3.19 we show the time series of rebound from dated beaches near the Angerman River, in Sweden. The best-fit curve depicted has a timescale τ of 3.8 ka: within 3.8 ka of the removal of the load, 1/e or roughly 37% of the rebound had occurred. The implied mantle viscosity may be calculated by solving the equation for the timescale for viscosity: $\mu = \Delta\rho g R \tau$. For $R = 1000$ km, $g = 9.8$ m^2/s, and the density difference of 3300–917, or roughly 2300 kg/m^3, the implied viscosity is $\mu = 3\times10^{21}$ Pa-s (see Andrews, 1968; Walcott, 1972; Cathles, 1975; Peltier and Andrews, 1976; Peltier *et al.*, 1986). In Figure 3.20 we show results from Paulson *et al.* (2005) in which the structure of mantle viscosity is inferred from data sets of this sort.

This analysis is quite simplified. The glacial rebound problem has been repeatedly revisited as more data

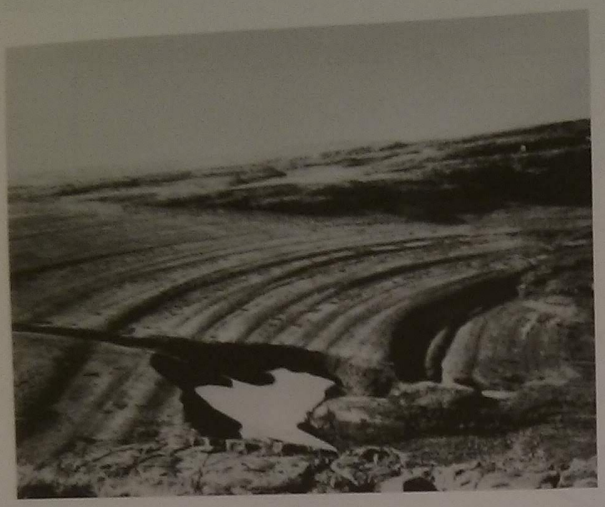

Figure 3.18 Flight of raised beaches tucked in the northwest sector of the Richmond Gulf Peninsula, Quebec, on the southeastern coast of Hudson Bay, near the site of maximum ongoing uplift of land due to post-glacial rebound (photograph by Claude Hillaire-Marcel, Université du Quebec à Montreal, with permission to reproduce).

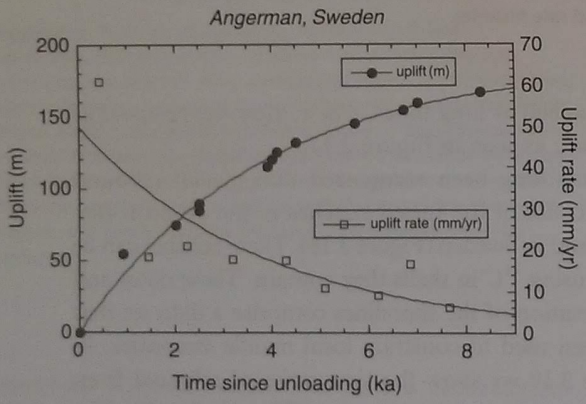

Figure 3.19 Rebound of Angerman River area, Sweden, in the aftermath of the demise of the Fennoscandian ice sheet. Data from dated shorelines. Boxes: uplift rates derived from differencing elevation and age data. The curves shown are the expected asymptotic exponential solution derived in the text for a site within the footprint of removed load. Same best-fit timescale for elevation data (3.77 ka) is used to fit rebound rate data. Note that the modern rate of uplift is about 5 mm/yr.

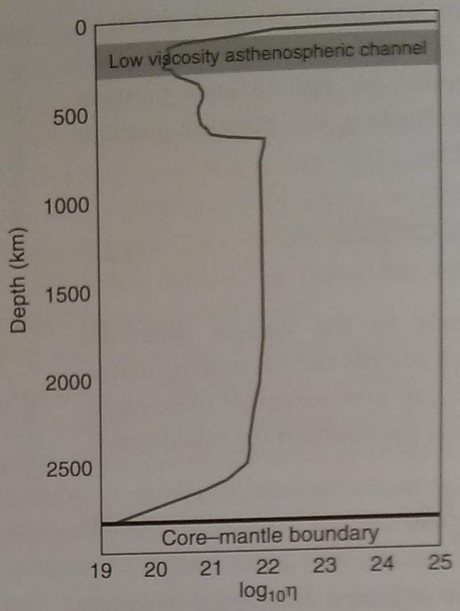

Figure 3.20 Profile of viscosity of the Earth's mantle showing low-viscosity "channel" in the upper mantle beneath the very high viscosity (rigid) lithosphere, relatively uniform viscosity in the lower mantle, and decline in viscosity at the core–mantle boundary. Note the logarithmic scale for the viscosity. Structure is constrained by numerous observations, including glacio-eustatic rebound histories around the globe (redrawn from Paulson *et al.*, 2005, Figure 3, with permission from Wiley-Blackwell Publishing).

have been assembled. Most recent work (e.g., Peltier, 2004; Paulson *et al.*, 2005; Mitrovica and Forte, 2004) acknowledges the complexity of the spatial and temporal pattern of loading, and the potential for both horizontal and vertical structure in the viscosity of the mantle to alter the simple patterns. The data now used to constrain this viscosity structure include the raised beaches already discussed, the modern tide gage records of the world's coastlines both inside and outside the loads, the tilting of the Great Lakes (deduced from lake level records on the north and south sides of the lake), gravity data from the GRACE satellite that documents the uplift rate over the entire region, and so on.

Note the two-way nature of the problem we have just treated. The elevations of the geomorphic features, here raised beaches, have allowed a calculation of an important geophysical number, the viscosity of the mantle, demonstrating their utility as probes of mantle viscosity. Just as importantly, the geomorphologist must be aware that the rearrangement of loads on the surface of the Earth incites a deep Earth response resulting in a deflection of the surface whose amplitude may be important for certain processes, which will be delayed relative to the loading by a time constant of several thousand years, determined by mantle viscosity.

Mantle flow and its influence on topography

While we commonly attribute much of the detail of the world's topography to the action of plate tectonics, and focus specifically on the margins of plates, where orogeny and volcanoes produce topography to be attacked by geomorphic processes, the effects of mantle convection are felt even in the interiors of continents. The details of the mantle-driven processes and their manifestation on the surface of the Earth are presently being debated. This is healthy, and will result in a rapid evolution of our thought about how the deep Earth influences the Earth's surface. The focus over the last half-century has been on horizontal tectonics, and its role in the formation of the mountain ranges of the world. The plate tectonic theory so pervaded the literature that the evidence for very broad scale vertical motions of the surface has been largely neglected. Pure vertical motion did not fit the new paradigm of horizontal plate motions translating into vertical motion. Only in the last decade has this problem re-emerged as a reasonable target for geodynamicists. In the interests of covering in this chapter the full panoply of geophysical processes of importance to geomorphology, here we briefly summarize an array of connections between deep Earth (mantle) and surface processes that should serve as catalysts for future study. These include the flow field set up within the mantle by motion of slabs in the mantle, and the tractions this can set up on the base of the lithosphere (called "dynamic topography"); the foundering of dense crustal roots from beneath mountain ranges; the gooshings of the asthenosphere over large distances in response to changing ice and water loads on the Earth's surface; and the motion of the lower crust in response to pressure gradients set up by the topography itself.

Dynamic topography

Recall that the timescale for a lithospheric slab to reach the core–mantle boundary, at 3000 km depth, is of the order of 100 million years if the vertical speed of the slab is 3 cm/yr (3×10^{6}m/3×10^{-2} m/yr $= 10^{8}$ years). These long timescales result in a very long legacy for the influence of lithospheric slabs on the Earth's surface. As we have discussed, a subducting slab of lithosphere sinks within the surrounding mantle because it is negatively buoyant – its mean density is higher than that of the surrounding mantle. The motion of this slab through the mantle incites a flow within the mantle, the detailed geometry of which depends upon the dip of the slab, the viscosity of the mantle, and so on. This flow inevitably affects the top surface, or the overlying lithosphere, by exerting a suction on it – a distribution of downward normal forces. This downward pull generates a huge dimple in the lithosphere, as depicted in Figure 3.21. The time and length scales of this deflection of the lithosphere are important. As you might guess, the horizontal scales are continental in size – they are dictated by the horizontal dimensions of the downgoing slab. The timescales are also set by the activity of the downgoing slab, but importantly involve as well the viscosity of the mantle (see for example the simulations in Figure 3.22). The higher the viscosity of a fluid, the longer it will take to respond to changes in the forces acting upon it. In the case of the Earth's upper mantle, the viscosity is so high that the timescales are of the order of tens of millions of years. This means that it might take 30 million years for the dimple to be produced as a subducting plate slides beneath a continental mass, and likewise it will take 30 million years for the dimple to decay away, or rebound, after the back edge of the slab passes by. But how deep might this dimple be? It is the vertical scales of the deflection that are surprising; they are of the order of a kilometer. This scale alone makes this phenomenon worthy of consideration by geomorphologists, as the mean

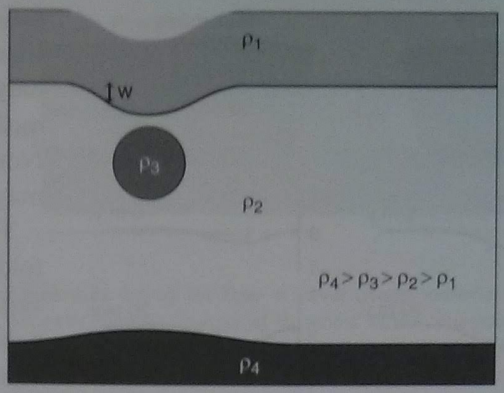

Figure 3.21 The essence of dynamic topography. Mantle density anomaly, here spherical, imposes flow in mantle interior that in turn deforms other density interfaces in the system (inspired by Davies, 1999, Figure 8.5).

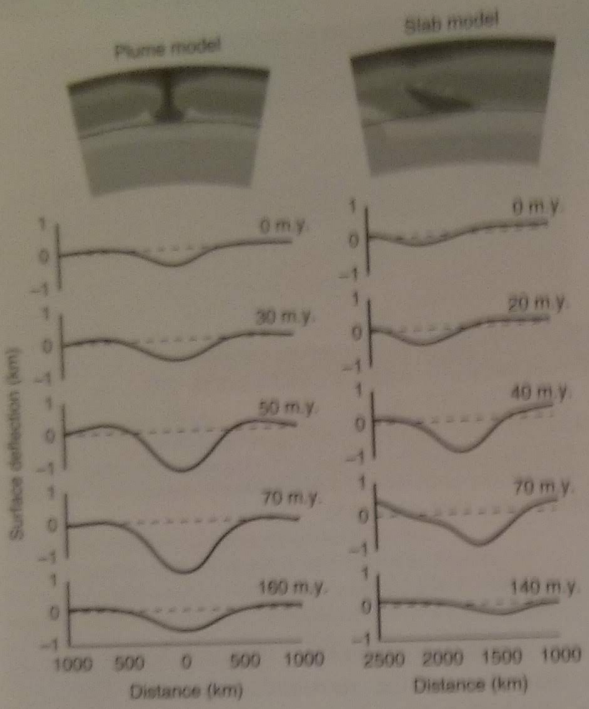

Figure 3.22 Dynamic topography over a rising plume (left) and a sinking slab (right), shown at different times in the calculation. Top cross section shows initial conditions for the models (= 0 Ma). Note the vertical scale of the deflection is of the order of 1 km (from Pysklywek and Mitrovica, 1998, Figures 2 and 3).

elevation of a continent (the so-called continental freeboard) is only about 800 m. During subduction of a plate beneath a continent, its interior could potentially be pulled beneath sea level, inciting deposition of marine sediments there, and upon cessation of subduction, this region ought to pop back up above sea level. In the absence of any knowledge of this process, one would falsely attribute such continental flooding to a rise in global sea level.

But how do we know this happens? How do we untangle the records of eustatic changes in sea level from those of dynamic topography associated with subduction? Close attention to the rock record is the key; where subtle tiltings of rock packages on subcontinental scales can be demonstrated (Mitrovica *et al.*, 1989), and evidence of synchroneity of eustatic sea level highstands with the deposition of these sediments is lacking, the finger can be pointed at large-scale mantle dynamics. Note that the tilts we are talking about here are small. They may be roughly scaled by the maximum vertical deflection (1 km) divided by the horizontal scale of the deflection (several thousand kilometers), meaning tilts of a few times 10^{-4}. Examples of continental flooding that may be attributed to dynamic topography can be seen in the rock records of the western interior seaway of North America, and in Australia. Present examples may include Indonesia (e.g., Gurnis, 2001).

The impact on geomorphic processes is severalfold. First, as we will see, rivers run across the land surface until they reach a stable water surface, either a lake or the ocean, which serves as a baselevel. Dynamic topography clearly can affect greatly the location of the coastline on a continent. Second, rivers transport sediment and incise into bedrock at rates that are dictated in part by the local slope of the river. River slopes can be quite subtle, ranging from a few meters per kilometer (0.001 for mountain streams) to a few centimeters per kilometer (10^{-5}, e.g., the Amazon). For big rivers, then, the scale of the tilting can be comparable to the river's slope, meaning that it could be either enhanced significantly, or reduced significantly (even reversed!) by this continental-scale process, depending upon the direction of the river flow, the orientation of the downgoing slab, and whether the subducting slab is just beginning to pass beneath the river, or just finishing. Finally, given that we are talking about a kilometer of vertical motion, one can imagine that the geomorphic processes active on existing topography will change as it passes from one elevation band to another. Both the precipitation forcing many geomorphic processes, and the vegetation that acts as a strong determinant of the type of geomorphic process change dramatically with elevation.

Topographic oozing of the Tibetan Plateau margin

In a landmark article, Marin Clark and Wicki Royden proposed that the smooth topographic ramp leading from southeastern China up to the Tibetan Plateau resulted from the oozing of hot lower crustal material from beneath the Plateau (Clark and Royden, 2000). This ramp contrasts sharply with the abrupt topographic front of the Himalayas that bounds the plateau to the south, visible in Figure 3.23. The physics of the problem is identical to that we have just introduced in the glacial rebound problem.

The analysis of Clark and Royden follows and simplifies an earlier model of the deformation of the

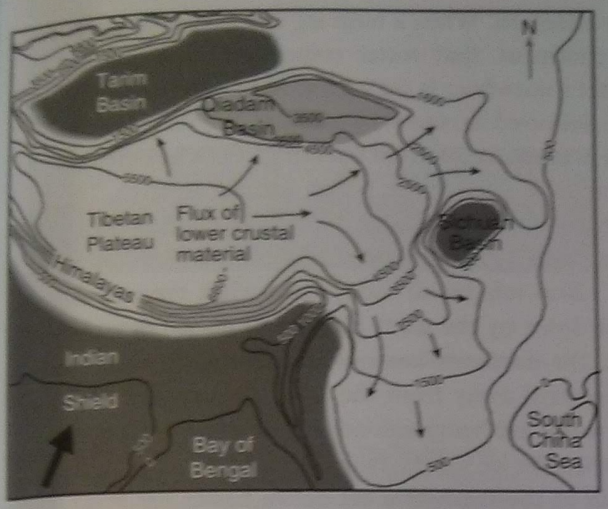

Figure 3.23 Map of Tibetan Plateau and surrounding lowlands, showing proposed direction of transport of lower crustal material from beneath plateau. Note the broad topographic ramp to the SE, and its contrast with the abrupt topographic front imposed by the Himalayas to the south of the plateau (from Clark and Royden, 2000, Figure 5).

Tibetan Plateau as a whole (Shen *et al*., 2000). Viscous lower crust (in this case) is being driven down a channel by a pressure gradient (Figure 3.24). The chief difference is that the channel through which the lower crust is being driven is unbounded – material is not being gooshed into or out of a cylinder but into a slot of effectively infinite length. We emphasize that whether the hypothesis is right or wrong (and there is indeed some support for it in river incision along this ramp (Schoenbohm *et al*., 2006)), their treatment can be understood using the same physics we have been exploring in this section.

We depict their proposed system in Figure 3.24. The rate of change in thickness of the lower crustal channel is determined by the gradient in the discharge of lower crustal material down the channel. In other words,

$$\frac{\partial z}{\partial t} = \frac{\partial h}{\partial t} = -\frac{\partial Q}{\partial x} \tag{3.27}$$

where h is the thickness of the channel, and Q is the discharge of viscous material along it. Again, the discharge, Q, is the volume of material per unit time per unit width of channel [= L^3/LT or L^2/T]. Since the thickness of upper crust above the viscous channel, h_o, does not change with time, the rate of change

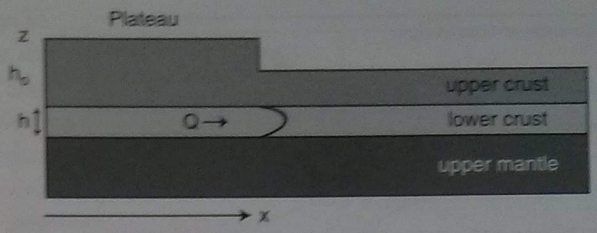

Figure 3.24 Set-up for flow of lower crustal material from beneath Plateau. Change of thickness of the low-viscosity channel, h, will result from gradients in the discharge of lower crustal material. Pressure driving the flow is tied to the thickness of the upper crust, h_o, which is non-uniform due to thickening of crust to form the Tibetan Plateau.

of elevation of the surface, z, simply follows the rate of change of thickness in the channel. It is, however, important that the thickness of crust h_o does vary in space. It is the thickened crust beneath the Tibetan Plateau that leads ultimately to its heating, which in turn leads to its reduction in viscosity and hence tendency to flow.

As in the rebound case, the discharge in the viscous channel is calculated from the integral of the velocity profile,

$$Q = \int_0^h U(z)\mathrm{d}z = -\frac{1}{12\mu}\frac{\partial p}{\partial x}h^3 \tag{3.28}$$

While at first the pressure gradient is set by the gradient in thickness of upper crust, gradients in lower crustal thickness will begin to play a role as it evolves:

$$\frac{\partial p}{\partial x} = \rho_c g \frac{\partial [h_o + h]}{\mathrm{d}x} \tag{3.29}$$

Inserting this expression into the statement of conservation of volume in the channel results in

$$\frac{\partial h}{\partial t} = \frac{\rho_c g}{12}\frac{\partial \left[\dfrac{h^3}{\mu}\dfrac{\partial (h_o + h)}{\partial x}\right]}{\partial x} \tag{3.30}$$

For now let's assume that the viscosity of the lower crust is uniform, so that we may pull it out of the derivative. Taking the derivative of the remaining product results in two terms:

$$\frac{\partial h}{\partial t} = \frac{\rho_c g}{12\mu}\left[h^3\left(\frac{\partial^2 h_o}{\partial x^2} + \frac{\partial^2 h}{\partial x^2}\right) + 3h^2\left\{\left(\frac{\partial h}{\partial x}\right)^2 + \frac{\partial h_o}{\partial x}\frac{\partial h}{\partial x}\right\}\right] \tag{3.31}$$

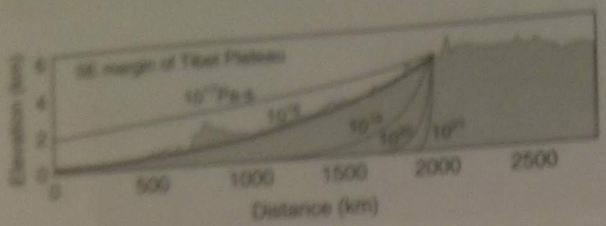

Figure 3.25 Topographic profile of ramp leading from Tibetan Plateau to the SE. Lines show solution for expected profile given an assumed viscosity of the lower crust channel (redrawn from Clark and Royden, 2000, Figure 4a).

Taking the leading term in this expression, dominated by h^3, leaves us with the simpler

$$\frac{\partial h}{\partial t} = \frac{\rho_c g h^3}{12\,\mu}\left[\left(\frac{\partial^2 h_o}{\partial x^2}\right) + \left(\frac{\partial^2 h}{\partial x^2}\right)\right] = \kappa\left[\frac{\partial^2 h_o}{\partial x^2} + \frac{\partial^2 h}{\partial x^2}\right] \tag{3.32}$$

The first term corresponds to a couplet of source–sink associated with the non-changing but non-uniform thickness distribution of the upper crust. The second term then acts to smear out this constant source, leading to the thickening of the lower crust (and associated inflation of topography) on the lengthening ramp, and simultaneous deflation of the lower crust below the edge of the Plateau. This is a diffusion equation, analogous to the one derived in our treatment of thermal problems except for this spatially distributed source term. The analogy is made explicit here by assigning an effective diffusivity, κ, to the collection of terms in front of the curvature. This constant reflects the efficiency with which changes in thickness occur. As expected, this efficiency is low when the viscosity is high, and is greatly enhanced when the channel is thick; the collection h^3/μ is difficult to disentangle.

Clark and Royden present results reproduced in Figure 3.25, based upon calculations assuming a channel thickness h of 15 km. Given this choice of channel thickness, the best-fitting viscosity of the lower crustal material is 10^{18} Pa-s.

Gooshing of mantle across the continental edge

We have talked about gooshing the mantle about by ice loads, and gooshing the lower crust by topographic loads. There is at least one other case worthy of our attention. When a huge ice sheet is constructed on a continent, that water comes from somewhere and that somewhere is the ocean. It gets there circuitously, delivered as snow by storms, but its ultimate source is evaporation from the ocean. So when the ice sheet volume is large the ocean volume is small. To give this a scale, at the Last Glacial Maximum some 20 thousand years ago, sea level was drawn down about 120 m relative to today. Just when the land is pushed down by the giant plunger of an ice sheet or two in the northern hemisphere, forcing mantle to flow outward away from the load, the ocean basins of the world are being unloaded. The converse is also true: when the ice sheets dwindle, mantle rushes back in, while at the same time the ocean basins are being loaded up, and mantle should be pushed away from them. Consider then a continental margin well away from any ice load. The variations in the ocean load adjacent to the continental margin should drive a gooshing of the mantle back and forth across the continental margin. Let's marry the two examples we have discussed so far, the ice load and the topographic ooze, and sprinkle in a periodic variation in the system to construct a model of this situation. Our goal is to assess the amplitude of the effect on the topography of the edge of the continent, and the distance inland over which this signal declines.

Assume a viscous channel in the upper mantle, beneath a uniform crust. Consider the simplest case of a very steep continental margin, in which the full 120 m swing of sea level does not cause significant lateral migration of a coastline. This is shown in Figure 3.26. Now allow sea level to vary sinusoidally with a fixed amplitude, Δh_{sea} and period, P:

$$h_{sea} = h_{sea} + \Delta h_{sea}(\sin(2\pi t/P)) \tag{3.33}$$

This variation in sea level translates into a variable pressure at the depth of the mantle channel, which in turn drives variation in the pressure gradient in the channel that causes transport of mantle. In addition, the thickness variation in the mantle then can drive flow as well, as the mean pressure in the thicker channel is greater than that in the thinner portion of the channel.

The conservation of fluid in the mantle channel is identical to the one we wrote for the Tibetan lower crustal ooze (Equation 3.10), as is the equation for lateral discharge of mantle. What differs is the pressure field driving flow, which now includes that of the dynamic oceanic load. The pressure is therefore

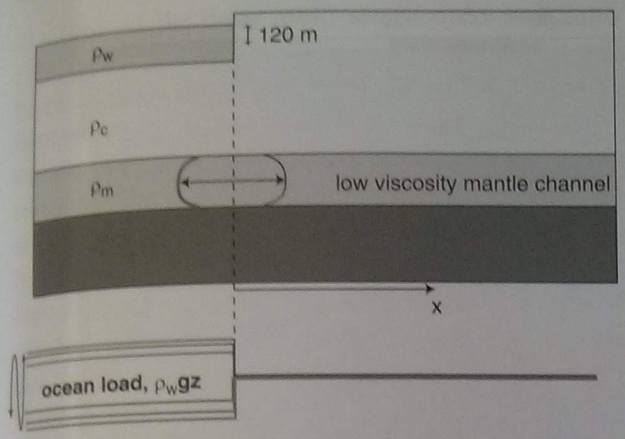

Figure 3.26 Schematic diagram illustrating the possible transport of mantle in a low-viscosity channel in response to oscillating sea level. The ocean load varies with sea level, which in the Pleistocene has varied by 120 m between glacial lowstands and interglacial highstands with periods of 20–100 ka. At highstands (light lines), mantle is forced from beneath the ocean load toward the interior of the continents (light velocity profile), while at lowstands (bold lines), mantle will be pushed toward the ocean basins (bold velocity profile). Our goal is to predict the resulting pattern of thickening of the channel, and the consequent raising or lowering of the land surface.

$$P = \rho_w g h_{sea} + \rho_c g h_c + \rho_m g(h/2) \tag{3.34}$$

When we acknowledge these contributions from all components of the load, the discharge becomes

$$Q = -\frac{1}{12\mu}\frac{dp}{dx}h^3 = -\frac{h^3}{12\mu}\left[\frac{d(\rho_w g h_{sea} + \rho_c g h_c + \rho_m g(h/2))}{dx}\right] \tag{3.35}$$

Because the thickness of the crust does not vary in time, and it is largely uniform in space in this problem, we drop this middle term. The statement for conservation of volume in the mantle channel then becomes

$$\frac{\partial h}{\partial t} = \frac{\rho_c g}{12\mu}\left\{h^3\left[\left(\frac{\partial^2 h_o}{\partial x^2}\right) + \left(\frac{\partial^2 h}{\partial x^2}\right)\right] + 3h^2\left[\left(\frac{\partial h}{\partial x}\right)^2 + \frac{\partial h}{\partial x}\frac{\partial h_o}{\partial x}\right]\right\} \tag{3.36}$$

This formulation explicitly acknowledges that the thickness of the channel, h, varies, which in turn causes variations in the discharge through the strong nonlinear h^3 dependence.

We have used a numerical model to explore the behavior of the system when forced with a 120 m oscillation in sea level. Results are shown in Figure 3.27. The system displays a diffusive behavior. It displays both an exponential decay of amplitude with distance from the margin, and a phase lag, much like the solution for temperature within a half space when forced by oscillation of the surface temperature (e.g., Gold and Lachenbruch, 1973; Turcotte and Schubert, 2002). In the thermal case, the length scale that dictates both the decay rate and the time lag is set by the square root of the thermal diffusivity and the period of the oscillation:

$$L = \sqrt{\frac{\kappa P}{\pi}} \tag{3.37}$$

The same appears to be the case in this system. Numerical experiments show that the penetration of the effect into the continent indeed depends upon

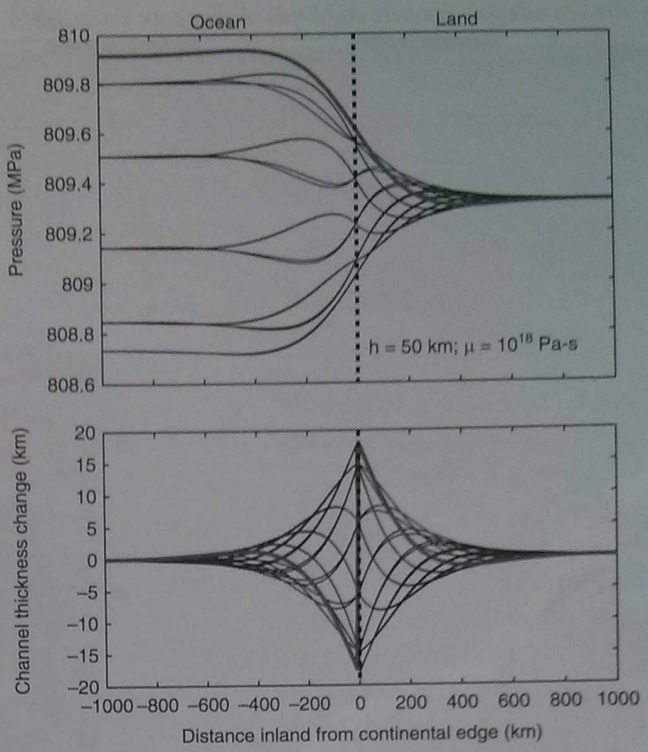

Figure 3.27 Elevation changes associated with periodic variations in sea level. (a) Pressure field calculated in upper-mantle channel at 10 times within a sinusoidal variation in sea level with period 20 ka, full amplitude 120 m (two oscillations shown). (b) Mantle channel thickness change driven by gradients in discharge of viscous channel material. This should result in elevation changes in the overlying landscape that extends hundreds of kilometers from the continental margin. Last time stamp (bold line) corresponds to sea level highstand.

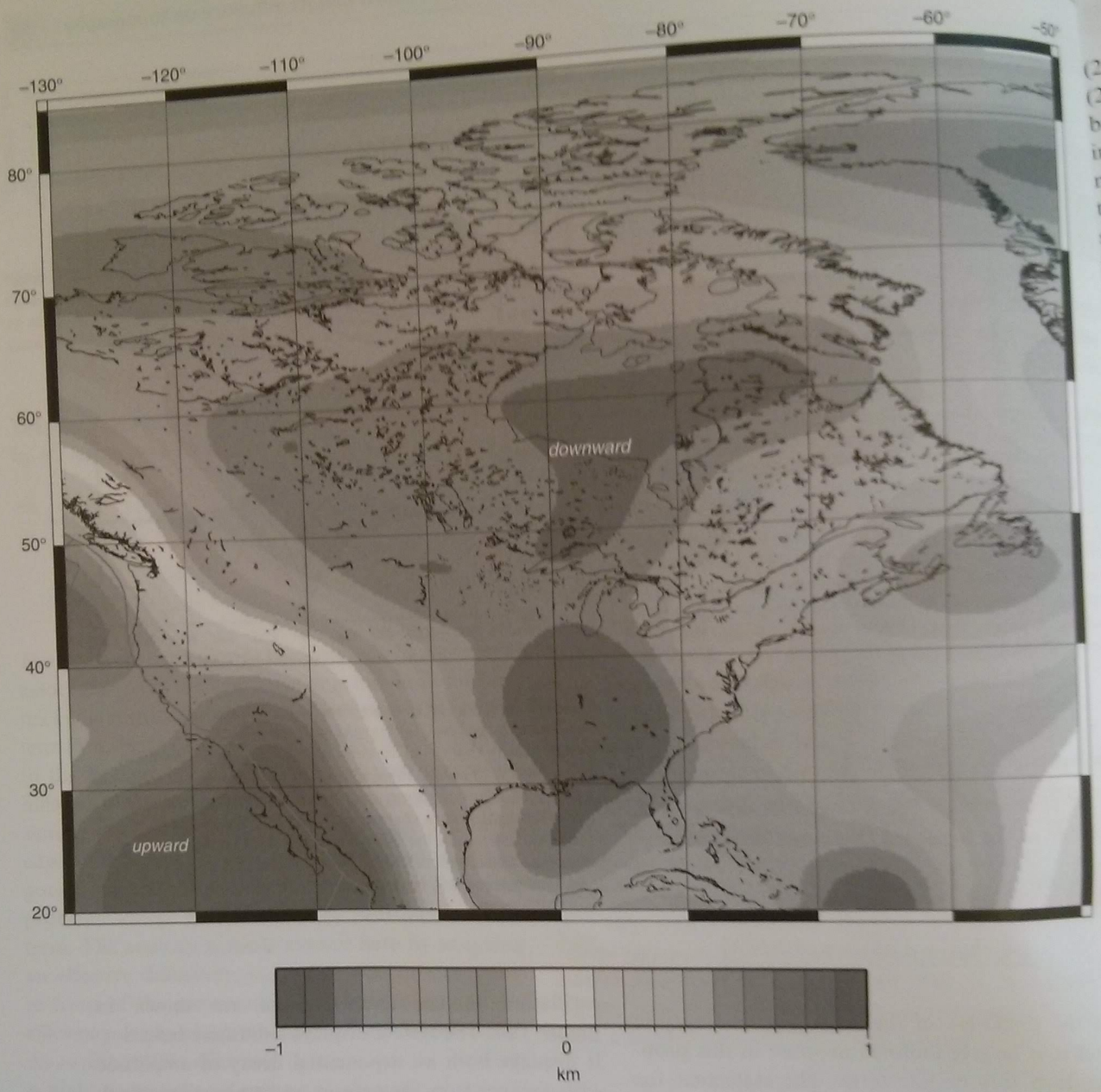

Figure 3.28 Vertical deflection of the North American lithosphere associated with the mantle flow field. The flow field is calculated from buoyancy forces set up by the density structure of the mantle, which is in turn constrained by seismic velocity structure (tomography). Note the amplitude is of the order of 1 km over central North America (reproduced from Forte *et al.*, 2007, Figure 2, with permission from the American Geophysical Union).

both the period of the oscillation and those variables that take the place of the diffusivity:

$$\kappa = \frac{\rho g h^3}{12\mu} \tag{3.38}$$

While this problem has yet to be fully exploited, we challenge the reader to look for hints that this gooshing of the mantle across the continental edge occurs. It seems to the authors that the geomorphic signal of this phenomenon will be best displayed where large rivers approach the coastline. Large rivers have small slopes. For example, the slope of the Amazon is around 1 cm/km, or 10^{-5}, while that of the Mississippi is perhaps a few times this

(2×10^{-5} on the delta itself; see Syvitski and Saito (2007)). The smaller the slope, the more likely it will be tweaked by the small tilts of the continental edge imposed by the movement of mantle across the margin. The maximum tilts in the case we have illustrated are about 15 m/300 km, or 5×10^{-5}; given the slopes of major rivers as they approach the coast, this tilt is worthy of discussion. Note also that a topographic sag comes and goes well inland of the margin – 500 km inland in the case we have illustrated – and that the sagging is out of phase with adverse tilt at the margin.

In working this problem (more or less as a teaser) we have not accounted for the rigidity of the lithosphere above the channel, which will serve to smooth any sharp gradients in the predicted thickness of the mantle channel. These occur at the continental margin. We also note that the larger effect on a river draining the continent is the more obvious and dramatic oscillation of the baselevel. During glacial times these major rivers seek to join an ocean (baselevel) that is 120 m below present, and should incise their margins as they seek that level. The greater hope to find the effect we have illustrated comes instead from its signal far inland from the margin, and in any temporal lag of the signal. After all, sea level reached its present highstand roughly 6000 years ago, while the high viscosity of the mantle channel should result in continued, ongoing warping of the margin.

In this section we have explored a few impacts of mantle physics on the overlying topography. These examples serve not only to illustrate another application of the principles of conservation, but to alert the geomorphologist that what happens deep in the Earth does indeed matter to its surface. These deep gooshings constitute the largest length scale processes to which the Earth's surface is subjected.

Calculation of the effects of large-scale mantle flow field on the surface of the Earth is now a growing subfield within geophysics. Here it is the motions of the cold negatively buoyant plates, and the upwellings of warmer mantle that exert tractions on the base of the lithosphere. One such calculation is shown in Figure 3.28 over North America. The magnitude of the effect is of the order of a kilometer, while the wavelengths over which these surface deflections occur are thousands of kilometers, and the timescales over which they change are tens of millions of years. These are surely subtle signals, but could have profound effects on the inundation history of continents, and on long-term evolution of drainage systems. They should not be overlooked in any attempt to understand long-term evolution of continental scale topography.

Summary

In this chapter we have introduced topographic features and geologic processes that could influence the deflection of the Earth's surface at scales so large that they involve the mantle in some fashion. Large wavelength loads on the Earth's surface (topography in the crust, ice, ocean) are supported not by the strength of the lithosphere but by buoyancy provided by the high density of the mantle. The timescales for response to changes in loads, and that set the rate at which mantle moves about beneath topography, are determined by the viscosity of that portion of the mantle involved.

The lithospheric plates themselves should be perceived as the rigid lids to a convecting mantle. They represent a rheological boundary layer. Given the strong dependence of rheology on temperature, the problem of plate thickness and its evolution translates into a thermal problem. We introduced the conservation of heat equation and the process of conduction by which heat moves in the lithosphere. The resulting diffusion equation could be solved for the thickness of the cooled boundary layer as a function of time since the top was exposed to the 4 °C base of the ocean at the spreading center. The lithosphere thickens as the square root of time. As any material cools it contracts and becomes more dense. The mean density of the lithosphere is therefore higher – by about 3% – than the underlying asthenosphere. Given this density contrast and the pattern of plate thickness, we could quantitatively explain the bathymetry of the world's oceans using an isostatic

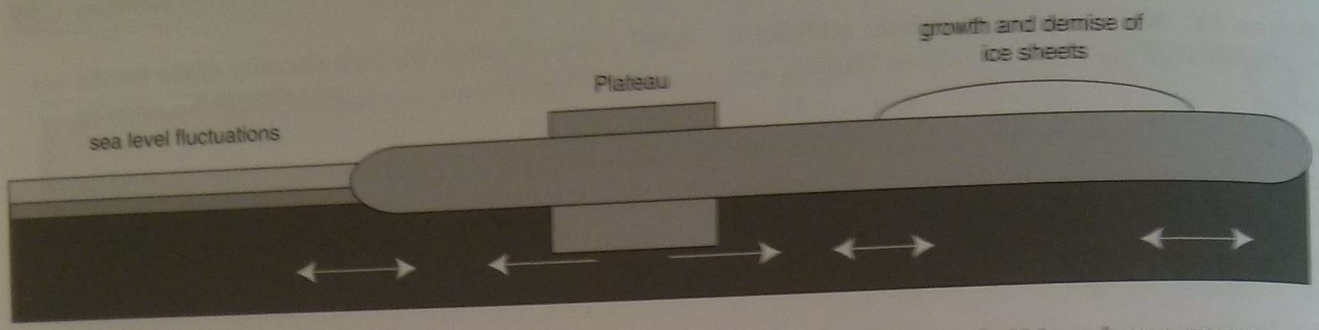

Figure 3.29 Summary diagram of the response of the mantle to a variety of Earth surface loads, each of which produces a pressure gradient in the underlying material. If the loads are emplaced for long enough, and the viscosity of the underlying material is weak enough to flow on these timescales, they will result in flow that in turn raises or lowers the surrounding landscape. Long-term growth of plateaus induces mantle or upper crustal flow away from the high topography. Other loads such as lakes and ice sheets are transient; they come and go, producing flow first away from the emplaced load, and then back under when it vanishes.

balance. As the ocean floors make up roughly two-thirds of the surface of the Earth, this calculation takes us a long way toward understanding the topography of the Earth.

We introduced briefly a simple model for the motion of the lithospheric plates. The roughly 10 cm/yr speeds of the plates could be amazingly well predicted by a theory in which the dense plates are falling downward through a dense, viscous mantle. While quite simplistic, the calculation nonetheless hints at what material properties of the mantle control these rates – the thermal diffusivity that controls the thickening rate of a plate, the coefficient of thermal contraction that controls the associated densification of the plate, and the mantle viscosity that controls the resistance of the mantle to shearing motions, and hence the drag on the plate as it descends.

Despite its importance not only in governing plate rates but also setting the response times to changes in surface loads, the viscosity of the mantle is difficult to measure. We have introduced several large-scale experiments Nature has performed for us in the form of the growth and demise of ice sheets and large lakes that provide a constraint on mantle viscosity. These are summarized in Figure 3.29. In most of these cases, the experiment involves deflection of some geomorphic marker on the Earth's surface that we know should have been horizontal at the time of formation. In most cases these are shorelines. The subsequent deflection of these horizontal markers, and their ages, has been a target of geomorphic study for more than a century.

We also discussed several examples of 1000 km scale deflections of the Earth's surface that are currently thought to have resulted from mantle (or deep crustal) dynamics. These are also shown in Figure 3.29, and include (1) continental-scale deflection of the surface by tractions on the base of the lithosphere associated with the flow field induced by slabs in the upper mantle, (2) the "oozing" of deep crustal material from beneath the edge of the Tibetan Plateau, driven by the pressure gradient set up by the great contrast in topography, and (3) the pumping of mantle back and forth across the continental margin associated with sea level oscillations in the ice ages.

Note that in treating this material we have employed the principle of conservation in at least two ways. We first encounter it in developing an equation for the conservation of heat, and second in developing the equation for conservation of mantle in a viscous channel. In both cases we find that the rate of change of the quantity of concern (heat, mantle volume) depends upon spatial gradients in the flux of that quantity. This forces us to acknowledge what governs the fluxes. In the case of heat in the lithosphere, this is conduction, represented by Fourier's law, and in the case of the mantle it is viscous fluid flow. We will encounter both of these again in this book, but more importantly we will see further examples of the utility of the conservation equation.

Problems

1. Calculate the fraction of an iceberg's total thickness that is above the surface of the ocean. Assume that the densities of ocean water and ice are 1003 and 917 kg/m^3, respectively. Please show a diagram of the situation, and be careful about the balance you set up.

   Now observe an ice cube in a glass of water as it melts, and plot both the root and the freeboard as functions of time. Plot their ratio as a function of time.

2. Calculate the expected deflection of the lithosphere beneath a thick ice sheet. Assume that the ice sheet is 4000 m thick, and that ice has a density of 917 kg/m^3. (The Antarctic Ice Sheet is roughly this thick at its maximum thickness.) The thickness of the crust (of density 2700 kg/m^3) beneath the center of the ice sheet and the region outside of it is the same. The density of the upper mantle that gooshes out of the way to allow this deflection of the surface is 3300 kg/m^3. How far down is the rock depressed beneath the load of the ice?

3. How much does the exposed land area change (a) during a sea level drop of 150 m and (b) during a sea level highstand of 500 m? Report your answers as fractions of the Earth's surface area that are land.

4. Assuming a continental crustal thickness of 25 km, an oceanic crustal thickness of 5 km, and an ocean depth of 4 km, calculate the continental freeboard using reasonable assumptions for continental crustal, oceanic crustal, mantle, and ocean densities.

5. Now consider what will happen to the maximum elevations of the land when V-shaped valleys are chopped throughout the landmass, extending down to sea level. Assume that the valleys take up the entire landscape, and that the tips of the ridges between them are not eroded. How much will the ridges rise? (*Hint:* scale this by the depth of the valleys or, equivalently, the relief of the landscape.)

6. *Oceanic lithospheric thickness.* In this chapter, we discussed the square root of age dependence of oceanic lithospheric thickness, and how this controls the bathymetric profile across an ocean basin. As we have seen, this collapses to a simple equation for ocean depth:

   $$D = D_0 + A\sqrt{\kappa t}$$

   where D is the ocean depth in m, D_0 the depth at the spreading ridge in m, t is the age of the lithosphere in years, and κ is the thermal diffusivity of the lithosphere.

   Given this equation, and the plot of ocean depth vs. age for the first 80 Ma for the North Pacific from Sclater's work (Figure 3.2), calculate a value for the dimensionless constant, A. Assume a reasonable thermal diffusivity of 1 mm^2/s. (*Hint*: watch out for units here, as the age of the lithosphere is given on the plot in millions of years (Ma). To make the answer for

A dimensionless, you will have to convert the diffusivity into m^2/yr and the age into years.)

7. *Heat flow in the Basin and Range*. In the Basin and Range province of the western USA the heat flow at the Earth's surface is considerably enhanced. In a 300 m-deep borehole in Owens Lake in the eastern California portion of the Basin and Range, the temperature increases by 18 °C from the surface to the base of the borehole. The conductivity of the materials is 4 W/(m K).

   What is the heat flux (also sometimes called the heat flow) at the surface of the Earth? Express this first in W/m^2, and then in heat flow units (HFU, where 1 HFU = 41.84 mW/m^2). Note that the worldwide average heat flow is 1.67 HFU.

8. *Thermal profile in and beneath an ice sheet*. Consider a portion of the East Antarctic Ice Sheet that is 2 km thick (in places it is significantly more than this). The mean annual surface temperature is −55 °C. The heat flux is 54 mW/m^2, which is a decent average for Antarctica. The thermal conductivity of ice is 2.2 W/(m K), and that of the underlying bedrock is 3.5 W/(m K).
   (i) Calculate and then plot the steady-state geotherm for this location, taking the temperature profile down into the underlying rock by 2 km. Assume no heat production from radioactivity takes place.
   (ii) At what depth into the bedrock does the temperature of the rock rise above the freezing point of water?

9. *Thought question*. Consider a hypothetical world of the same dimensions as Earth, in which plate speeds are steady at 10 cm/yr, and on which one mega-continent 6000 km across exists. At time 0 the continent splits in half along a N–S rift extending from the north pole to the south pole, while a subduction zone is simultaneously born along the western edge of the western half of the continent. How long would it take before a major continent–continent collision occurs? (This timescale governs a very long cycle of mega-continent assemblies.)

10. *Thought question*. How would the world differ if the plate rates were twice as fast? (*Hint*: focus first at least on the shapes and depths of ocean basins.) How much might sea level change due to such a speed-up?

11. *Thought question*. Review the means by which information from geomorphology has been used to evaluate the character of the mantle (for example, its viscosity).

Further reading

Cathles, L. M., 1975, *The Viscosity of the Earth's Mantle*, Princeton, NJ: Princeton University Press, 386 pp.

A classic treatise on what we know about the viscosity of the Earth's mantle. While we now know much more than then, the book still illustrates well the types of data one assembles in these problems, and provides a snapshot of our knowledge in the early 1970s.

Davies, G., 1999, *Dynamic Earth: Plates, Plumes and Mantle Convection*, Cambridge: Cambridge University Press, 458 pp.

This textbook addresses the physics necessary to understand quantitatively the dynamics of the Earth with particular focus on the mantle. Davies lays out the thermal and fluid mechanics pieces at several levels of complexity, making his arguments accessible to a wide array of students.

Turcotte, D. L. and G. Schubert, 2002, *Geodynamics*, 2nd edition, Cambridge: Cambridge University Press, 456 pp.

This textbook on geophysics serves as an excellent introduction to quantitative geophysics, with tendrils that reach into geomorphology and planetary science.